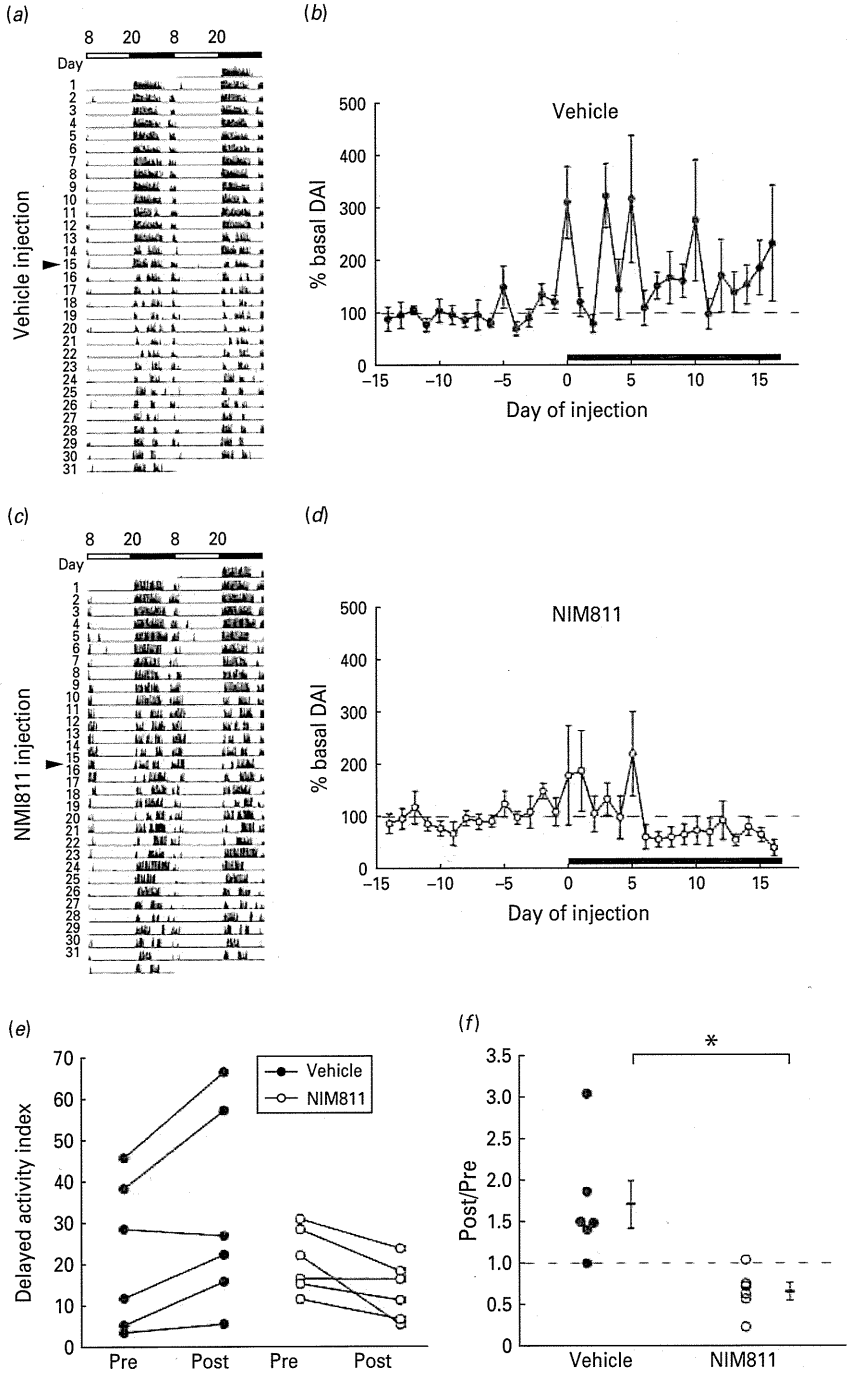

Fig. 3. Effect of 40 mg/kg NIM811 on wheel-running activity in *mutPolg1* Tg mice. Individual activity record of (*a*) vehicle-treated or (*c*) NIM811-treated *mutPolg1* Tg mice. An arrowhead indicates the first day of injection (day 15). Standardized delayed activity index (DAI) of (*b*) vehicle-treated or (*d*) NIM811-treated *mutPolg1* Tg mice. DAI during (Post) the treatment was standardized by the mean value before the treatment (Pre). A broken line shows the basal activity level. Day 0 indicates the first day of injection. A horizontal bar represents the period of the drug injection. (*e*) Change of DAI of individual animals. The indices before the treatment was averaged for 14 d (Pre: days −14 to −1) and after the treatment for 10 d (Post: days 7–16). (*f*) Effect of the vehicle or NIM811 treatment on DAI. The effect of drug treatment was estimated by the ratio of the index values before (Pre) and after (Post) treatment. * $p<0.05$ (Aspin–Welch's modified t test). Values indicate mean ± S.E.M. ($n=6$ for each group). A broken line shows the averaged level of DAI before the treatment.

Mitochondria isolated from cells overexpressing *BCL-2* were more resistant to PTP opening (Shimizu *et al.* 1998). Further, mitochondria from Tg mice with overexpression of *BCL-2* showed a higher membrane potential after treatment with Ca^{2+} (Shimizu *et al.* 1998). In both studies, overexpression of *BCL-2* prevented apoptotic processes. The mRNA expression and protein levels of Bcl-2 were increased in myocytes of heart-specific *mutPolg1* Tg mice (Mott *et al.* 2001; Zhang *et al.* 2005). The increased Bcl-2 was speculated to be an adaptive protective response (Mott *et al.* 2004). These findings suggest that inhibition of PTP opening, in general, might be a therapeutic strategy against BD.

Recent studies demonstrated that CypD immunoreactivity in the hippocampus was primarily localized in neurons rather than in astrocytes (Mouri *et al.* 2009; Naga *et al.* 2007). CypD is abundant in synaptic mitochondria compared to non-synaptic mitochondria (Naga *et al.* 2007). Mitochondria contribute to Ca^{2+} buffering in the synaptic terminal (Billups & Forsythe, 2002; Kim *et al.* 2005). Release of glutamate and acetylcholine was decreased in CypD knockout mice (Mouri *et al.* 2009). Taken together, these finding suggest that CypD down-regulation may also affect local synaptic dysfunction.

Interestingly, up-regulation of *SFPQ*, as shown in Table 2, was also reported in the other set of post-mortem frontal cortices of BD patients (Nakatani *et al.* 2006). Based on the gene expression analysis of DBP (D-box binding protein) knockout mice and the convergent functional genomics approach, Le-Niculescu and colleagues suggested that *SFPQ* is a novel candidate gene for BD (Le-Niculescu *et al.* 2008). A protein, polyprimidine tract-binding protein-associated splicing factor (PSF) encoded by *SFPQ* has been identified as regulating gene expression of a mitochondrial phosphate carrier (Iacobazzi *et al.* 2005), which is also involved in PTP opening (Leung *et al.* 2008). Expression of *SFPQ* was enriched through brain development and highly detected in differentiated neurons rather than in non-neuronal cells in zebrafish (Lowery *et al.* 2007). Immunoreactivity of PSF was also apparent in the brains and was much stronger at the stage of neuronal differentiation (Chanas-Sacre *et al.* 1999). This suggests that *SFPQ* could play a role in neuron-specific splicing or transcriptional regulation even in the adult brain. Additionally, the increased cell death by low level of *SFPQ* expression at the embryonic stage in zebrafish indicated that PSF protein normally suppresses apoptosis (Lowery *et al.* 2007). In our data, *SFPQ* was up-regulated in the brains of Tg mice and patients, which exerts an anti-apoptotic effect. This result is in line with the biological function of CypD down-regulation. Thus, it is plausible to assume that mutant *Polg1* causes accumulation of mtDNA deletions, which exerts compensatory changes of *PPIF* and *SFPQ*. The functional significance of the up-regulation of *SFPQ* should be clarified. Recently, it has been reported that an aberrant splicing mechanism is relevant to the pathophysiology of affective disorders (Glatt *et al.* 2009; Watanuki *et al.* 2008).

In the present results, 3/39 (7.6%) human probes corresponding to the altered mice probes were also differentially expressed in the patients. Because 682/11920 (5.7%) probes were differentially expressed in patients, the number of altered genes is not significantly larger than that expected by chance ($p=0.48$ by Fisher's exact probability test). Thus, it cannot be excluded that the overlap between the mouse gene profiling and the human one is due to chance. However, the role of down-regulation of *Ppif* was supported by the pharmacological analysis of Ppif *in vivo* using Tg mice.

In the present study, we also found that GR mRNA was down-regulated in the *mutPolg1* Tg mice (Table 2). Considering that down-regulation of GR has been reported in several animal models of depression (Boyle *et al.* 2005; Herman *et al.* 1995; Kitraki *et al.* 1999), we think this finding further supports the validity of our model as an animal model of mood disorders.

In summary, we found that down-regulation of CypD with up-regulation of *SFPQ* was the common molecular signature in the mouse model and post-mortem brains of BD patients. A CypD inhibitor, NIM811, improved the behavioural phenotype of the mice. This suggests that CypD is a promising drug target for BD. This is the first application of the neuron-specific *mutPolg1* Tg mice in the study of drug development.

Acknowledgements

Post-mortem brains were donated by the Stanley Foundation Brain Collection, courtesy of Drs Michael B. Knable, E. Fuller Torrey, Maree J. Webster, and Robert H. Yolken. We are grateful to staff members of the BSI Research Resource Center for technical assistance and for microarray analysis. We also thank BoldFace Editors, Inc., for language editing of the manuscript. This work was supported by grants to the Laboratory for Molecular Dynamics of Mental Disorders, RIKEN BSI, a Grant-in-Aid from the Japanese Ministry of Health and Labor, and

Grants-in-Aid from the Japanese Ministry of Education, Culture, Sports, Science and Technology. NIM 811 was provided by Novartis Pharma.

Statement of Interest

None.

References

Baines CP, Kaiser RA, Purcell NH, Blair NS, *et al.* (2005). Loss of cyclophilin D reveals a critical role for mitochondrial permeability transition in cell death. *Nature* **434**, 658–662.

Basso E, Fante L, Fowlkes J, Petronilli V, *et al.* (2005). Properties of the permeability transition pore in mitochondria devoid of cyclophilin D. *Journal of Biological Chemistry* **280**, 18558–18561.

Billups B, Forsythe ID (2002). Presynaptic mitochondrial calcium sequestration influences transmission at mammalian central synaipses. *Journal of Neuroscience* **22**, 5840–5847.

Boyle MP, Brewer JA, Funatsu M, Wozniak DF, *et al.* (2005). Acquired deficit of forebrain glucocorticoid receptor produces depression-like changes in adrenal axis regulation and behavior. *Proceedings of the National Academy of Sciences USA* **102**, 473–478.

Chanas-Sacre G, Mazy-Servais C, Wattiez R, Pirard S, *et al.* (1999). Identification of PSF, the polypyrimidine tract-binding protein-associated splicing factor, as a developmentally regulated neuronal protein. *Journal of Neuroscience Research* **57**, 62–73.

Chen G, Zeng WZ, Yuan PX, Huang LD, *et al.* (1999). The mood-stabilizing agents lithium and valproate robustly increase the levels of the neuroprotective protein bcl-2 in the CNS. *Journal of Neurochemistry* **72**, 879–882.

Corson TW, Woo KK, Li PP, Warsh JJ (2004). Cell-type specific regulation of calreticulin and Bcl-2 expression by mood stabilizer drugs. *European Neuropsychopharmacology* **14**, 143–150.

Dager SR, Friedman SD, Parow A, Demopulos C, *et al.* (2004). Brain metabolic alterations in medication-free patients with bipolar disorder. *Archives of General Psychiatry* **61**, 450–458.

Dennis Jr. G, Sherman BT, Hosack DA, Yang J, *et al.* (2003). DAVID: database for annotation, visualization, and integrated discovery. *Genome Biology* **4**, P3.

Du H, Guo L, Fang F, Chen D, *et al.* (2008). Cyclophilin D deficiency attenuates mitochondrial and neuronal perturbation and ameliorates learning and memory in Alzheimer's disease. *Nature Medicine* **14**, 1097–1105.

Ferreira MA, O'Donovan MC, Meng YA, Jones IR, *et al.* (2008). Collaborative genome-wide association analysis supports a role for *ANK3* and *CACNA1C* in bipolar disorder. *Nature Genetics* **40**, 1056–1058.

Forte M, Gold BG, Marracci G, Chaudhary P, *et al.* (2007). Cyclophilin D inactivation protects axons in experimental autoimmune encephalomyelitis, an animal model of multiple sclerosis. *Proceedings of the National Academy of Sciences USA* **104**, 7558–7563.

Glatt SJ, Chandler SD, Bousman CA, Chana G, *et al.* (2009). Alternatively spliced genes as biomarkers for schizophrenia, bipolar disorder and psychosis: a blood-based spliceome-profiling exploratory study. *Current Pharmacogenomics and Personalized Medicine* **7**, 164–188.

Hansson MJ, Mattiasson G, Mansson R, Karlsson J, *et al.* (2004). The nonimmunosuppressive cyclosporin analogs NIM811 and UNIL025 display nanomolar potencies on permeability transition in brain-derived mitochondria. *Journal of Bioenergetics and Biomembranes* **36**, 407–413.

Herman JP, Adams D, Prewitt C (1995). Regulatory changes in neuroendocrine stress-integrative circuitry produced by a variable stress paradigm. *Neuroendocrinology* **61**, 180–190.

Hiroi T, Wei H, Hough C, Leeds P, *et al.* (2005). Protracted lithium treatment protects against the ER stress elicited by thapsigargin in rat PC12 cells: roles of intracellular calcium, GRP78 and BCL-2. *Pharmacogenomics Journal* **5**, 102–111.

Huang da W, Sherman BT, Lempicki RA (2009). Systematic and integrative analysis of large gene lists using DAVID bioinformatics resources. *Nature Protocols* **4**, 44–57.

Iacobazzi V, Infantino V, Costanzo P, Izzo P, *et al.* (2005). Functional analysis of the promoter of the mitochondrial phosphate carrier human gene: identification of activator and repressor elements and their transcription factors. *Biochemical Journal* **391**, 613–621.

Iwamoto K, Bundo M, Kato T (2005). Altered expression of mitochondria-related genes in postmortem brains of patients with bipolar disorder or schizophrenia, as revealed by large-scale DNA microarray analysis. *Human Molecular Genetics* **14**, 241–253.

Jeong MR, Hashimoto R, Senatorov VV, Fujimaki K, *et al.* (2003). Valproic acid, a mood stabilizer and anticonvulsant, protects rat cerebral cortical neurons from spontaneous cell death: a role of histone deacetylase inhibition. *FEBS Letters* **542**, 74–78.

Kakiuchi C, Iwamoto K, Ishiwata M, Bundo M, *et al.* (2003). Impaired feedback regulation of XBP1 as a genetic risk factor for bipolar disorder. *Nature Genetics* **35**, 171–175.

Kasahara T, Kubota M, Miyauchi T, Noda Y, *et al.* (2006). Mice with neuron-specific accumulation of mitochondrial DNA mutations show mood disorder-like phenotypes. *Molecular Psychiatry* **11**, 577–593.

Kato T (2007). Mitochondrial dysfunction as the molecular basis of bipolar disorder: therapeutic implications. *CNS Drugs* **21**, 1–11.

Kato T (2008). Molecular neurobiology of bipolar disorder: a disease of 'mood-stabilizing neurons'? *Trends in Neurosciences* **31**, 495–503.

Kato T, Kato N (2000). Mitochondrial dysfunction in bipolar disorder. *Bipolar Disorders* **2**, 180–190.

Kato T, Takahashi S, Shioiri T, Inubushi T (1993). Alterations in brain phosphorous metabolism in bipolar disorder detected by in vivo ^{31}P and ^{7}Li magnetic resonance spectroscopy. *Journal of Affective Disorders* **27**, 53–59.

Kato T, Takahashi S, Shioiri T, Murashita J, *et al.* (1994). Reduction of brain phosphocreatine in bipolar II disorder detected by phosphorus-31 magnetic resonance spectroscopy. *Journal of Affective Disorders* **31**, 125–133.

Kim MH, Korogod N, Schneggenburger R, Ho WK, *et al.* (2005). Interplay between Na^+/Ca^{2+} exchangers and mitochondria in Ca^{2+} clearance at the calyx of held. *Journal of Neuroscience* **25**, 6057–6065.

Kitraki E, Karandrea D, Kittas C (1999). Long-lasting effects of stress on glucocorticoid receptor gene expression in the rat brain. *Neuroendocrinology* **69**, 331–338.

Korde AS, Pettigrew LC, Craddock SD, Pocernich CB, *et al.* (2007). Protective effects of NIM811 in transient focal cerebral ischemia suggest involvement of the mitochondrial permeability transition. *Journal of Neurotrauma* **24**, 895–908.

Kubota M, Kasahara T, Nakamura T, Ishiwata M, *et al.* (2006). Abnormal Ca^{2+} dynamics in transgenic mice with neuron-specific mitochondrial DNA defects. *Journal of Neuroscience* **26**, 12314–12324.

Le-Niculescu H, McFarland MJ, Ogden CA, Balaraman Y, *et al.* (2008). Phenomic, convergent functional genomic, and biomarker studies in a stress-reactive genetic animal model of bipolar disorder and co-morbid alcoholism. *American Journal of Medical Genetics. Part B, Neuropsychiatric Genetics* **147B**, 134–166.

Leung AW, Varanyuwatana P, Halestrap AP (2008). The mitochondrial phosphate carrier interacts with cyclophilin D and may play a key role in the permeability transition. *Journal of Biological Chemistry* **283**, 26312–26323.

Li JZ, Vawter MP, Walsh DM, Tomita H, *et al.* (2004). Systematic changes in gene expression in postmortem human brains associated with tissue pH and terminal medical conditions. *Human Molecular Genetics* **13**, 609–616.

Lowery LA, Rubin J, Sive H (2007). Whitesnake/sfpq is required for cell survival and neuronal development in the zebrafish. *Developmental Dynamics* **236**, 1347–1357.

Luvisetto S, Basso E, Petronilli V, Bernardi P, *et al.* (2008). Enhancement of anxiety, facilitation of avoidance behavior, and occurrence of adult-onset obesity in mice lacking mitochondrial cyclophilin D. *Neuroscience* **155**, 585–596.

Mbye LH, Singh IN, Sullivan PG, Springer JE, *et al.* (2008). Attenuation of acute mitochondrial dysfunction after traumatic brain injury in mice by NIM811, a non-immunosuppressive cyclosporin A analog. *Experimental Neurology* **209**, 243–253.

Millay DP, Sargent MA, Osinska H, Baines CP, *et al.* (2008). Genetic and pharmacologic inhibition of mitochondrial-dependent necrosis attenuates muscular dystrophy. *Nature Medicine* **14**, 442–447.

Mott JL, Zhang D, Chang SW, Zassenhaus HP (2006). Mitochondrial DNA mutations cause resistance to opening of the permeability transition pore. *Biochimica et Biophysica Acta* **1757**, 596–603.

Mott JL, Zhang D, Freeman JC, Mikolajczak P, *et al.* (2004). Cardiac disease due to random mitochondrial DNA mutations is prevented by cyclosporin A. *Biochemical and Biophysical Research Communications* **319**, 1210–1215.

Mott JL, Zhang D, Stevens M, Chang S, *et al.* (2001). Oxidative stress is not an obligate mediator of disease provoked by mitochondrial DNA mutations. *Mutation Research* **474**, 35–45.

Mouri A, Noda Y, Shimizu S, Tsujimoto Y, *et al.* (2009). The role of cyclophilin D in learning and memory. *Hippocampus* **20**, 293–304.

Naga KK, Sullivan PG, Geddes JW (2007). High cyclophilin D content of synaptic mitochondria results in increased vulnerability to permeability transition. *Journal of Neuroscience* **27**, 7469–7475.

Nakagawa T, Shimizu S, Watanabe T, Yamaguchi O, *et al.* (2005). Cyclophilin D-dependent mitochondrial permeability transition regulates some necrotic but not apoptotic cell death. *Nature* **434**, 652–658.

Nakatani N, Hattori E, Ohnishi T, Dean B, *et al.* (2006). Genome-wide expression analysis detects eight genes with robust alterations specific to bipolar I disorder: relevance to neuronal network perturbation. *Human Molecular Genetics* **15**, 1949–1962.

Nonaka S, Hough CJ, Chuang DM (1998). Chronic lithium treatment robustly protects neurons in the central nervous system against excitotoxicity by inhibiting N-methyl-D-aspartate receptor-mediated calcium influx. *Proceedings of the National Academy of Sciences USA* **95**, 2642–2647.

Palma E, Tiepolo T, Angelin A, Sabatelli P, *et al.* (2009). Genetic ablation of cyclophilin D rescues mitochondrial defects and prevents muscle apoptosis in collagen VI myopathic mice. *Human Molecular Genetics* **18**, 2024–2031.

Qing H, Xu H, Wei Z, Gibson K, *et al.* (2003). The ability of atypical antipsychotic drugs vs. haloperidol to protect PC12 cells against MPP^+-induced apoptosis. *European Journal of Neuroscience* **17**, 1563–1570.

Rasmussen A, Hjortrup A, Hansen B, Heslet L, *et al.* (1996). Induction of immunosuppression by microemulsion cyclosporine in liver transplantation. *Transplantation* **62**, 1031–1033.

Ravikumar R, McEwen ML, Springer JE (2007). Post-treatment with the cyclosporin derivative, NIM811, reduced indices of cell death and increased the volume of spared tissue in the acute period following spinal cord contusion. *Journal of Neurotrauma* **24**, 1618–1630.

Regenold WT, Phatak P, Marano CM, Sassan A, *et al.* (2009). Elevated cerebrospinal fluid lactate concentrations in patients with bipolar disorder and schizophrenia: implications for the mitochondrial dysfunction hypothesis. *Biological Psychiatry* **65**, 489–494.

Sakata A, Tamai I, Kawazu K, Deguchi Y, *et al.* (1994). *In vivo* evidence for ATP-dependent and P-glycoprotein-mediated transport of cyclosporin A at the blood-brain barrier. *Biochemical Pharmacology* **48**, 1989–1992.

Schinzel AC, Takeuchi O, Huang Z, Fisher JK, *et al.* (2005). Cyclophilin D is a component of mitochondrial permeability transition and mediates neuronal cell death after focal cerebral ischemia. *Proceedings of the National Academy of Sciences USA* **102**, 12005–12010.

Shimizu S, Eguchi Y, Kamiike W, Funahashi Y, *et al.* (1998). Bcl-2 prevents apoptotic mitochondrial dysfunction by regulating proton flux. *Proceedings of the National Academy of Sciences USA* **95**, 1455–1459.

Stork C, Renshaw PF (2005). Mitochondrial dysfunction in bipolar disorder: evidence from magnetic resonance spectroscopy research. *Molecular Psychiatry* **10**, 900–919.

Sullivan PG, Rabchevsky AG, Hicks RR, Gibson TR, *et al.* (2000). Dose-response curve and optimal dosing regimen of cyclosporin A after traumatic brain injury in rats. *Neuroscience* **101**, 289–295.

Suomalainen A, Majander A, Haltia M, Somer H, *et al.* (1992). Multiple deletions of mitochondrial DNA in several tissues of a patient with severe retarded depression and familial progressive external ophthalmoplegia. *Journal of Clinical Investigation* **90**, 61–66.

Tomita H, Vawter MP, Walsh DM, Evans SJ, *et al.* (2004). Effect of agonal and postmortem factors on gene expression profile: quality control in microarray analyses of postmortem human brain. *Biological Psychiatry* **55**, 346–352.

Waldmeier PC, Feldtrauer JJ, Qian T, Lemasters JJ (2002). Inhibition of the mitochondrial permeability transition by the nonimmunosuppressive cyclosporin derivative NIM811. *Molecular Pharmacology* **62**, 22–29.

Watanuki T, Funato H, Uchida S, Matsubara T, *et al.* (2008). Increased expression of splicing factor SRp20 mRNA in bipolar disorder patients. *Journal of Affective Disorders* **110**, 62–69.

Zhang D, Mott JL, Chang SW, Stevens M, *et al.* (2005). Mitochondrial DNA mutations activate programmed cell survival in the mouse heart. *American Journal of Physiology. Heart and Circulatory Physiology* **288**, H2476–2483.

Biochimica et Biophysica Acta 1807 (2011) 270–274

Contents lists available at ScienceDirect

Biochimica et Biophysica Acta

journal homepage: www.elsevier.com/locate/bbabio

Regional variation in mitochondrial DNA copy number in mouse brain

Satoshi Fuke [a], Mie Kubota-Sakashita [a], Takaoki Kasahara [a], Yasufumi Shigeyoshi [b], Tadafumi Kato [a,*]

[a] Laboratory for Molecular Dynamics of Mental Disorders, RIKEN Brain Science Institute, 2-1 Hirosawa, Wako, Saitama 351-0198, Japan
[b] Department of Anatomy and Neurobiology, Kinki University School of Medicine, 377-2 Ohno-Higashi, Osakasayama, Osaka 589-8511, Japan

ARTICLE INFO

Article history:
Received 3 August 2010
Received in revised form 10 November 2010
Accepted 30 November 2010
Available online 8 December 2010

Keywords:
Cerebellum
Copy number
Dopamine
mtDNA
Substantia nigra
Ventral tegmental area

ABSTRACT

Mitochondria have their own DNA (mitochondrial DNA [mtDNA]). Although mtDNA copy number is dependent on tissues and its decrease is associated with various neuromuscular diseases, detailed distribution of mtDNA copies in the brain remains uncertain. Using real-time quantitative PCR assay, we examined regional variation in mtDNA copy number in 39 brain regions of male mice. A significant regional difference in mtDNA copy number was observed ($P<4.8\times10^{-35}$). High levels of mtDNA copies were found in the ventral tegmental area and substantia nigra, two major nuclei containing dopaminergic neurons. In contrast, cerebellar vermis and lobes had significantly lower copy numbers than other regions. Hippocampal dentate gyrus also had a relatively low mtDNA copy number. This study is the first quantitative analysis of regional variation in mtDNA copy number in mouse brain. Our findings are important for the physiological and pathophysiological studies of mtDNA in the brain.

1. Introduction

Mitochondria play important roles in energy production, apoptosis, calcium signaling, as well as synaptic transmission, and neuroplasticity in neurons [1]. Mitochondrial dysfunction induces various mitochondrial diseases and may also be linked to neurodegenerative disorders, such as Parkinson's disease (PD), Alzheimer's disease, and Huntington's disease [2–4]. These mitochondrial dysfunctions can result from heteroplasmic mitochondrial DNA (mtDNA) mutations, including point mutations and deletions in mtDNA [4,5]. A mitochondrion contains a number of mtDNA copies, and mtDNA depletion also causes mitochondrial diseases [5–10]. It is possible that differences in mtDNA copy number among brain regions lead to association with region-dependent mitochondrial function and disease susceptibility. However, the distribution of mtDNA copies in the brain has not been studied in detail so far.

In the present study, we determined mtDNA copy number in 39 representative brain regions of adult mice using a micropunch technique and real-time quantitative PCR (qPCR). The results demonstrate that mtDNA is enriched in substantia nigra (SN) and the ventral tegmental area (VTA), where dopaminergic neurons are located.

2. Materials and methods

2.1. Animals

Male C57BL/6J mice were kept in the laboratory under light/dark conditions of 12 h:12 h (lights on at 8:00 a.m.). The laboratory was air-conditioned, and temperature and humidity were maintained at approximately 22–23 °C and 50–60%, respectively. From age 20 to 28 weeks, mice were individually housed in cages (24 cm wide × 11 cm deep × 14 cm high) equipped with a steel wheel (5 cm wide × 14 cm in diameter). All animal experiments were performed in accordance with the protocols approved by the Animal Experiment Committee of RIKEN (Wako, Saitama, Japan). All efforts were made to minimize the number of animals used and their suffering.

2.2. Micropunch

Transcardiac perfusion fixation was performed with 4% paraformaldehyde in phosphate-buffered saline (PBS), and then brains were immersed in PBS.

Slices (0.5 mm thick) of mouse brain were generated using a mouse brain matrix (Neuroscience, Tokyo, Japan), and 39 regions (Table 1, Fig. 1) were punched out bilaterally from the fixed slices under a stereomicroscope with a handmade microdissecting needle (gauge 0.5 mm), which has thinner wall than commercially available micropunchers, to pick up adjacent regions from one slice. The anatomical nomenclature is based on the atlas of Franklin and Paxinos

* Corresponding author. Tel.: +81 48 467 6949; fax: +81 48 467 6947.
E-mail address: kato@brain.riken.jp (T. Kato).

0005-2728/$ – see front matter © 2010 Elsevier B.V. All rights reserved.
doi:10.1016/j.bbabio.2010.11.016

Table 1
Micropunched 39 brain regions.

Brain area	Abbreviations	Brain region
Cerebral cortex	PrL-s	Prelimbic cortex–superficial layers
	PrL-de	Prelimbic cortex–deep layers
	IL-s	Infralimbic cortex–superficial layers
	IL-de	Infralimbic cortex–deep layers
	Cg	Cingulate cortex
	Motor-s	Motor cortex–superficial layers
	Motor-in	Motor cortex–intermediate layers
	Motor-de	Motor cortex–deep layers
	cc	Corpus callosum
Hippocampus	CA1	CA1
	CA2/CA3	CA2, CA3
	DG	Dentate gyrus
Amygdala	A Amy-m	Anterior amygdaloid complex–medial
	A Amy-l	Anterior amygdaloid complex–lateral
	P Amy-m	Posterior amygdaloid complex–medial
	P Amy-l	Posterior amygdaloid complex–lateral
Septum	LS	Lateral septal nucleus
Basal ganglia	Acb-core	Accumbens nucleus–core
	Acb-shell	Accumbens nucleus–shell
	CP-m	Caudate putamen–medial
	CP-l	Caudate putamen–lateral
	LGP	Lateral globus pallidus
Thalamus	VP	Ventral posterior thalamic nucleus
	PVT	Paraventricular nucleus of thalamus
	MD	Mediodorsal thalamic nucleus
	Hb	Habenular nucleus
	LG	Lateral geniculate body
	MG	Medial geniculate body
Hypothalamus	SCN	Suprachiasmatic nucleus
	SPZ-v	Subparaventricular zone–ventral part
	SPZ-do	Subparaventricular zone–dorsal part
	PV	Paraventricular hypothalamic nucleus
	LH	Lateral hypothalamic area
Midbrain	SN	Substantia nigra
	VTA	Ventral tegmental area
	IP	Interpeduncular nucleus
	PAG	Periaqueductal gray
Cerebellum	Cb-vermis	Cerebellar cortex–vermis
	Cb-lobe	Cerebellar cortex–lobe

(Fig. 1) [11]. After overnight incubation of each micropunched region in lysis buffer (1 punch/25 μl, 10 mM Tris–HCl, pH 8.0, 1 mM EDTA, pH 8.0, 0.5% Triton X-100, and 500 μg/ml proteinase K [Roche Applied Science, Mannheim, Germany]) at 55 °C, samples were incubated at 65 °C over 6 h to de-crosslink, followed by heat inactivation at 96 °C for 10 min and addition of an equal amount of 10 mM Tris–HCl (pH 8.0).

2.3. Real-time qPCR analysis

Real-time qPCR analysis was performed using the 7900HT Fast Real-Time PCR System (Applied Biosystems, Foster City, CA, USA) with SYBR Premix Ex Taq reagent (Takara Bio, Otsu, Japan) according to the manufacturer's instructions. Each PCR product was separately amplified from 2 μl of lysate of micropunched sample in a 10-μl reaction containing 5 μl of 2 × SYBR Premix and 0.2 μM of each primer.

For estimation of amounts of mtDNA in mice, the control region (D-loop) of mouse mtDNA was amplified using the primer pair D1 (5′-CCC AAG CAT ATA AGC TAG TAC-3′) and D2 (5′-ATA TAA GTC ATA TTT TGG GAA CTA C-3′). Using this primer set, the thermal cycling protocol used was 95 °C for 20 s, 55 °C for 20 s, 72 °C for 80 s for 30 cycles after an initial denaturation. In a preliminary experiment, the quantification using *COX1* or *ND4* region in mtDNA showed similar results to quantification using D-loop region, that is, lower copy number in cerebellum compared with frontal lobe, other cortices, and basal ganglia (Supplementary Figure 1). For determination of the amount of nuclear DNA, the *apoB* gene was used as a reference: 5′-CGT GGG CTC CAG CAT TCT A-3′ and 5′-TCA CCA GTC ATT TCT GCC TTT G-3′. In the case of amplification using these three primer sets, 40 cycles of two-step PCR followed: 95 °C for 10 s and 60 °C for 30 s after an initial denaturation at 95 °C for 1 min.

These real-time qPCRs were carried out in quadruplicate for all measurements. After confirmation of the single major peak representing the specific amplification with the melting curve, the quantities of each PCR product were calibrated by a linear regression model, using standard curves calculated between Ct values and the logarithm of concentrations of standard pCR2.1-TOPO plasmids (Invitrogen, Carlsbad, CA, USA) containing each PCR fragment. In every run, the high linearity (R^2>0.99) of the standard curves was verified by amplifications of each PCR product from dilution series of the plasmids made up to 10 ng by pCR2.1-TOPO plasmid. Ct values of all samples were within the linear range.

The relative number of mtDNA copies per cell was calculated as the normalized ratio of D-loop/*apoB* gene to a median value of 39 brain regions. In all samples examined, PCR products both of the D-loop in mtDNA and of the *apoB* gene in nuclear genome were amplified within the linear range of assays.

2.4. Statistical analysis

The results of quantitative experiments were analyzed by nonparametric tests after use of the Kolmogorov–Smirnov test for confirmation of a normal distribution. A two-tailed test was used for exploratory analysis. Statistical significance was determined using KyPlot 4.0 (KyensLab, Tokyo, Japan). Relative mtDNA copy numbers in several regions did not show a statistically normal distribution (Kolmogorov–Smirnov test, $P<0.05$). Therefore, we used nonparametric tests for detection of statistical significance among brain regions. To determine detailed significant regional differences in mtDNA copy number, we used the nonparametric multiple comparison Steel–Dwass test ($\alpha=0.05$).

3. Results

The average relative mtDNA copy number in the 39 brain areas was between 0.0847 and 2.54 (Fig. 1). There was a statistically significant regional variation in mtDNA copy number among the 39 brain regions (Kruskal–Wallis test, $P<4.8\times10^{-35}$) (Fig. 2). In VTA, the mtDNA copy number (median = 2.62, average ± SD = 2.54 ± 0.80) was significantly higher than in 24 other regions. The relative mtDNA copy number in SN (median = 2.12, average ± SD = 2.23 ± 0.65) was higher than in 19 other regions. Moreover, the interpeduncular nucleus (IP) showed a significantly higher mtDNA copy number (median = 1.76, average ± SD = 1.86 ± 0.53) than did 14 other brain regions.

In contrast, a significantly lower mtDNA copy number was observed in the anterior cerebellar lobe (Cb-lobe) (median = 0.0965, average ± SD = 0.0847 ± 0.0492) than in most other regions. MtDNA copy number in cerebellar vermis (Cb-vermis) (median = 0.0857, average ± SD = 0.144 ± 0.157) was lower than in 28 other brain regions. In the dentate gyrus (DG), mtDNA copy number (median = 0.321, average ± SD = 0.384 ± 0.196) was significantly lower than in 18 other brain regions.

In addition to these statistical differences, there were significant differences between caudate putamen–medial (CP-m) (median = 0.594, average ± SD = 0.567 ± 0.236) or habenular nucleus (Hb) (median = 0.325, average ± SD = 0.408 ± 0.284) and anterior amygdaloid complex–lateral (A Amy-l) (median = 1.31, average ± SD = 1.36 ± 0.48) or motor cortex–intermediate layers (Motor-in) (median = 1.31, average ± SD = 1.33 ± 0.40).

No significant differences were detected between other brain regions.

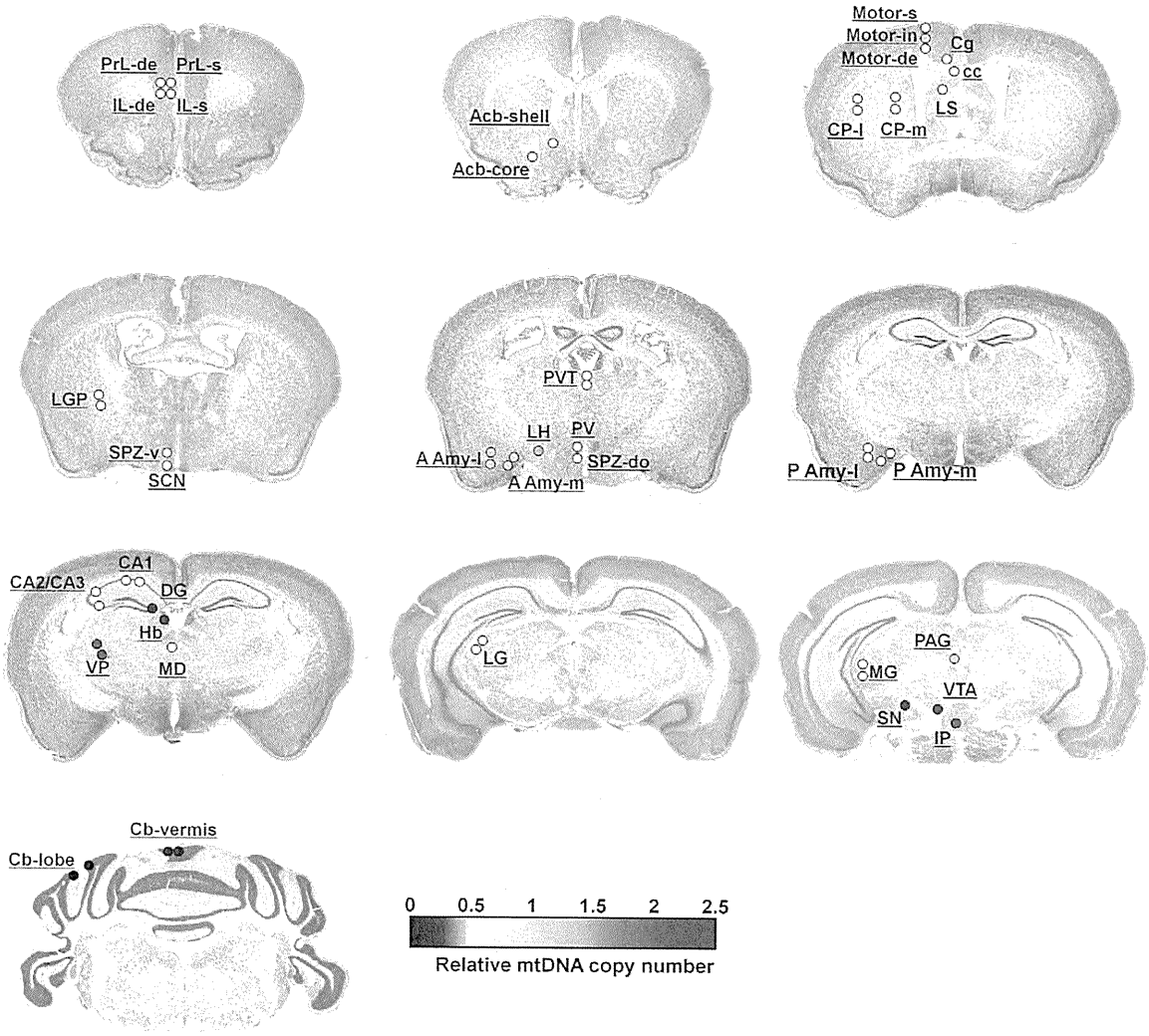

Fig. 1. Thirty-nine representative brain structures punched out bilaterally are shown in Nissl-stained coronal slices of a mouse brain. Regional variation of mitochondrial DNA (mtDNA) copy number is shown as a pseudo-color heat map. Abbreviations are expanded in Table 1.

4. Discussion

In this study, we first quantitatively demonstrated that there is a large regional variation in mtDNA copy number in the brain. Study results could be affected by regional variation in the neuron/glia ratio, if there is a difference in mtDNA copy number between neuron and glia. An *in situ* mtDNA hybridization study showed stronger signals from gray matter than from white matter in striate cortex of primates [12], and an *in situ* PCR study also showed stronger signals from neurons than from glial cells [13]. However, a study using qPCR analysis showed no statistically significant difference in mtDNA copy number between gray matter and white matter of human postmortem brains [14]. In addition, the mtDNA copy number in corpus callosum, containing mostly glial cells, was comparable to that in other brain regions in this study. The results of these quantitative analysis studies suggest that the 30-fold difference in mtDNA copy number between VTA and cerebellum cannot be solely accounted for by regional variation in neuron/glia ratio.

The highest mtDNA copy numbers were observed in VTA and SN, two major midbrain nuclei containing dopaminergic neurons. This finding might be relevant to the fact that mitochondrial dysfunction and mtDNA mutations are implicated in PD, caused by degeneration of dopaminergic neurons of SN [2,3,15]. PD is also a frequent complication of mitochondrial diseases [4,5]. Degeneration of VTA neurons is reported to be associated with depression [16], which is also a frequent comorbid condition of mitochondrial disease [5]. It remains unclear why VTA and SN contain particularly high copy number of mtDNA. It is plausible that vulnerability of mtDNA to oxidative stress resulting from the metabolism of dopamine in these two nuclei may be relevant to the present finding [17]. Meanwhile, it has recently been shown that high mtDNA copy number induces increased mtDNA deletion formation, which might be caused by increased mtDNA replication [18]. If high mtDNA copy number in SN indicates faster turnover, it might be relevant to the fact that SN is particularly susceptible to defects of the clearance of damaged mitochondria, due to mutations of Parkin and PINK1 [5,19,20].

On the other hand, cerebellar vermis and lobes had particularly low levels of mtDNA. The significantly lower mtDNA copy number in cerebellum is consistent with other reports that cerebellum showed lower level of mtDNA copies than several brain areas of rat or human [21,22]. A number of mitochondrial diseases associated with mtDNA depletion and mutations affect the cerebellum [4,5,23]. Although it is still unclear that both the regions with high mtDNA copy number such as SN and those with low copy number such as cerebellum are relevant to mitochondrial diseases, it would coincide with the fact that both depletion and increased copy number of mtDNA are reported to cause mitochondrial dysfunction [8,18]. It seems reasonable that mutation of

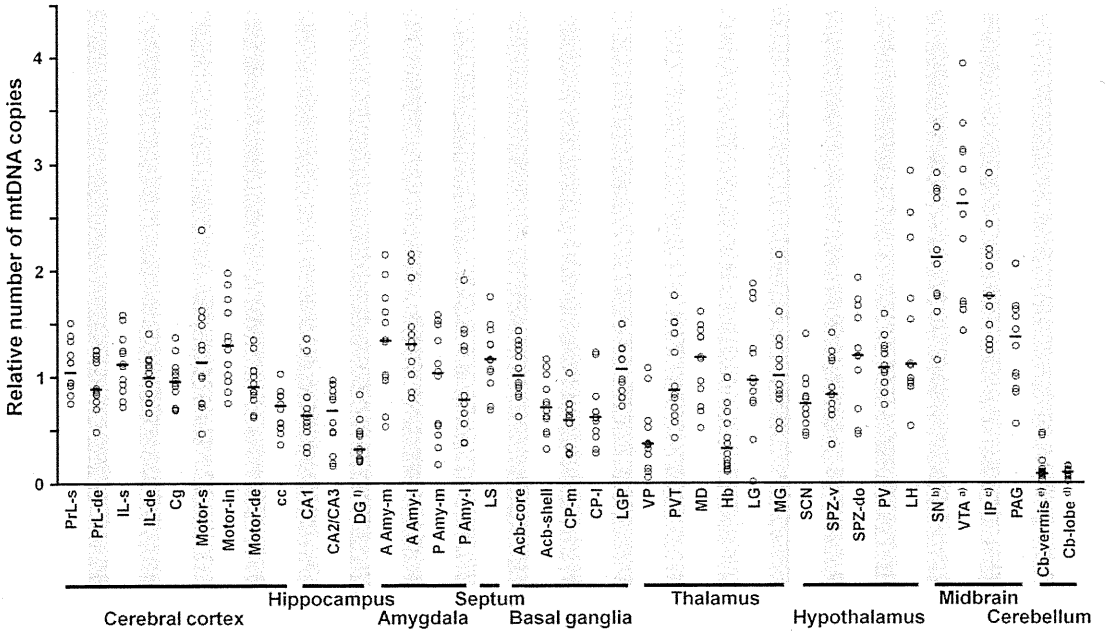

Fig. 2. Analysis of mtDNA copy number in 39 micropunched brain regions shows substantial regional variation. Each circle indicates one mouse ($n=12$). The vertical axis represents the estimated relative number of mtDNA copies to a median value of 39 brain regions. Group median values are indicated by horizontal bars. The horizontal axis represents each brain region. Differences among brain regions were observed (Kruskal–Wallis test, $P<4.8\times10^{-35}$). A multiple comparison using the Steel–Dwass test ($\alpha=0.05$) showed significant differences in mtDNA copy number among brain regions, as follows: (a) VTA>PrL-s, PrL-de, IL-s, IL-de, Cg, Motor-de, cc, CA1, CA2/CA3, DG, P Amy-m, Acb-core, Acb-shell, CP-m, CP-l, LGP, VP, MD, Hb, SCN, SPZ-v, PV, Cb-vermis, and Cb-lobe; (b) SN>PrL-s, PrL-de, IL-de, Cg, Motor-de, cc, CA1, CA2/CA3, DG, P Amy-m, Acb-shell, CP-m, CP-l, VP, Hb, SCN, SPZ-v, Cb-vermis, and Cb-lobe; (c) IP>PrL-de, IL-de, cc, CA2/CA3, DG, Acb-shell, CP-m, CP-l, VP, Hb, SCN, SPZ-v, Cb-vermis, and Cb-lobe; (d) Cb-lobe<PrL-s, PrL-de, IL-s, Il-de, Cg, Motor-s, Motor-in, Motor-de, cc, CA1, CA2/CA3, DG, A Amy-m, A Amy-l, P Amy-m, P Amy-l, Acb-core, Acb-shell, LS, CP-m, CP-l, LGP, PVT, MD, MG, SCN, SPZ-v, SPZ-do, PV, LH, SN, VTA, IP, and PAG; (e) Cb-vermis<PrL-s, PrL-de, IL-s, IL-de, Cg, Motor-s, Motor-in, Motor-de, cc, CA1, A Amy-m, A Amy-l, Acb-core, Acb-shell, LS, LGP, PVT, MD, MG, SCN, SPZ-v, SPZ-do, PV, LH, SN, VTA, IP, PAG; and (f) DG<PrL-s, IL-s, IL-de, Cg, Motor-in, Motor-de, A Amy-m, A Amy-l, Acb-core, LS, LGP, MD, PV, LH, SN, VTA, IP, and PAG. Abbreviations are expanded in Table 1.

mtDNA in smaller copy number can affect the mitochondrial function in the brain regions having lower copy number of mtDNA.

In the present study, we fixed the tissues with 4% paraformaldehyde, because it is difficult to capture more than one region at equal conditions from a frozen or fresh brain section due to its fragility. This approach also allowed us to identify brain structures clearly; we were able to pick up all brain regions from one animal at once. Moreover, we confirmed that paraformaldehyde fixation did not affect the linearity of quantification of each PCR product ($R^2>0.91$, Supplementary Figure 2) and relative amount of mtDNA per nucleus can be compared among brain regions using fixed samples. By introducing de-crosslinking, we could measure mtDNA copy number. This methodology made it possible to describe the distribution in detail.

Our findings on regional variation in mtDNA copy number in the brain provide important information on regional differences in vulnerability to mitochondrial dysfunction.

Supplementary materials related to this article can be found online at doi:10.1016/j.bbabio.2010.11.016.

Acknowledgements

We are grateful to the staff at the Divisions of Animal Experiments and Common Instrumentations in Research Resources Center, RIKEN Brain Science Institute (BSI), for technical assistance; Ms. Mizue Kametani for the care of mice used in the study; and the other members in our laboratory for valuable discussions.

This work was supported by grants from the Laboratory for Molecular Dynamics of Mental Disorders, RIKEN BSI; a Grant-in-Aid from the Japanese Ministry of Health and Labor; and Grants-in-Aid from the Japanese Ministry of Education, Culture, Sports, Science and Technology. S.F.'s research is supported by Grants-in-Aid for Young Scientists from the Japanese Ministry of Education, Culture, Sports, Science and Technology.

References

[1] D.C. Chan, Mitochondria: dynamic organelles in disease, aging, and development, Cell 125 (2006) 1241–1252.
[2] M. Baron, A.P. Kudin, W.S. Kunz, Mitochondrial dysfunction in neurodegenerative disorders, Biochem. Soc. Trans. 35 (2007) 1228–1231.
[3] M.F. Beal, Mitochondria take center stage in aging and neurodegeneration, Ann. Neurol. 58 (2005) 495–505.
[4] S. Dimauro, G. Davidzon, Mitochondrial DNA and disease, Ann. Med. 37 (2005) 222–232.
[5] A. Suomalainen, J. Kaukonen, Diseases caused by nuclear genes affecting mtDNA stability, Am. J. Med. Genet. 106 (2001) 53–61.
[6] R.K. Bai, C.L. Perng, C.H. Hsu, L.J. Wong, Quantitative PCR analysis of mitochondrial DNA content in patients with mitochondrial disease, Ann. NY Acad. Sci. 1011 (2004) 304–309.
[7] R.K. Bai, L.J. Wong, Simultaneous detection and quantification of mitochondrial DNA deletion(s), depletion, and over-replication in patients with mitochondrial disease, J. Mol. Diagn. 7 (2005) 613–622.
[8] S. Alberio, R. Mineri, V. Tiranti, M. Zeviani, Depletion of mtDNA: syndromes and genes, Mitochondrion 7 (2007) 6–12.
[9] W.C. Copeland, Inherited mitochondrial diseases of DNA replication, Annu. Rev. Med. 59 (2008) 131–146.
[10] C. Tzoulis, M. Papingji, T. Fiskestrand, L.S. Røste, L.A. Bindoff, Mitochondrial DNA depletion in progressive external ophthalmoplegia caused by POLG1 mutations, Acta Neurol. Scand. Suppl. 189 (2009) 38–41.
[11] K. Franklin, G. Paxinos, The Mouse Brain in Stereotaxic Coordinates, Academic Press, San Diego, CA, 1997.
[12] R.F. Hevener, M.T. Wong-Riley, Mitochondrial and nuclear gene expression for cytochrome oxidase subunits are disproportionately regulated by functional activity in neurons, J. Neurosci. 13 (1993) 1805–1819.
[13] S. Melov, J.A. Schneider, P.E. Coskun, D.A. Bennett, D.C. Wallace, Mitochondrial DNA rearrangements in aging human brain and in situ PCR of mtDNA, Neurobiol. Aging 20 (1999) 565–571.
[14] A. Blokhin, T. Vyshkina, S. Komoly, B. Kalman, Variations in mitochondrial DNA copy numbers in MS brains, J. Mol. Neurosci. 35 (2008) 283–287.
[15] A. Bender, K.J. Krishnan, C.M. Morris, G.A. Taylor, A.K. Reeve, R.H. Perry, E. Jaros, J.S. Hersheson, J. Betts, T. Klopstock, R.W. Taylor, D.M. Turnbull, High levels of mitochondrial DNA deletions in substantia nigra neurons in aging and Parkinson disease, Nat. Genet. 38 (2006) 515–517.
[16] R.M. Torack, J.C. Morris, The association of ventral tegmental area histopathology with adult dementia, Arch. Neurol. 45 (1988) 497–501.
[17] B. Halliwell, Reactive oxygen species and the central nervous system, J. Neurochem. 59 (1992) 1609–1623.

[18] E. Ylikallio, H. Tyynismaa, H. Tsutsui, T. Ide, A. Suomalainen, High mitochondrial DNA copy number has detrimental effects in mice, Hum. Mol. Genet. 19 (2010) 2695–2705.
[19] O. Rothfuss, H. Fischer, T. Hasegawa, M. Maisel, P. Leitner, F. Miesel, M. Sharma, A. Bornemann, D. Berg, T. Gasser, N. Patenge, Parkin protects mitochondrial genome integrity and supports mitochondrial DNA repair, Hum. Mol. Genet. 18 (2009) 3832–3850.
[20] N. Matsuda, S. Sato, K. Shiba, K. Okatsu, K. Saisho, C.A. Gautier, Y. Sou, S. Saiki, S. Kawajiri, F. Sato, M. Kimura, M. Komatsu, N. Hattori, K. Tanaka, PINK1 stabilized by mitochondrial depolarization recruits Parkin to damaged mitochondria and activates latent Parkin for mitophagy, J. Cell Biol. 189 (2010) 211–221.
[21] T. Frahm, S.A. Mohamed, P. Bruse, C. Gemünd, M. Oehmichen, C. Meissner, Lack of age-related increase of mitochondrial DNA amount in brain, skeletal muscle and human heart, Mech. Ageing Dev. 126 (2005) 1192–1200.
[22] S.C. McInerny, A.L. Brown, D.W. Smith, Region-specific changes in mitochondrial D-loop in aged rat CNS, Mech. Ageing Dev. 130 (2009) 343–349.
[23] M. Manto, D. Marmolino, Cerebellar disorders—at the crossroad of molecular pathways and diagnosis, Cerebellum 8 (2009) 417–422.

Neuroscience Research xxx (2011) xxx–xxx

Contents lists available at ScienceDirect

Neuroscience Research

journal homepage: www.elsevier.com/locate/neures

Survey of the effect of genetic variations on gene expression in human prefrontal cortex and its application to genetics of psychiatric disorders

Kazuya Iwamoto[a,b,*], Junko Ueda[a], Miki Bundo[a,b], Toshio Kojima[c,d], Tadafumi Kato[a,**]

[a] Laboratory for Molecular Dynamics of Mental Disorders, RIKEN Brain Science Institute, 2-1 Hirosawa, Wako, Saitama 351-0198, Japan
[b] Department of Molecular Psychiatry, Graduate School of Medicine, The University of Tokyo, 7-3-1 Hongo, Bunkyo-ku, Tokyo 351-0198, Japan
[c] Comparative Systems Biology Team, RIKEN Genomic Sciences Center, 1-7-22 Suehiro-cho, Tsurumi-ku, Yokohama 230-0045, Japan
[d] Research Equipment Center, Hamamatsu University School of Medicine, Shizuoka, Japan

ARTICLE INFO

Article history:
Received 25 January 2011
Received in revised form 24 February 2011
Accepted 24 February 2011
Available online xxx

Keywords:
Genetics
Postmortem brain
Microarray
Psychiatry

ABSTRACT

Identifying the genetic basis of gene expression variation in the human brain is important for understanding brain physiology and pathophysiology. We investigated the genetic basis of gene expression variation in human prefrontal cortex using single nucleotide polymorphisms (SNPs) and taking into consideration brain sample pH. From approximately 12,000 brain-expressed transcripts, we identified 187 *cis*-regulated transcripts. Some of the transcripts were identified as *cis*-regulated in the lymphoblastoid cells or lymphocytes, which suggests common *cis*-regulation across different tissues. Knowledge of genetic variations contributing to differences in gene expression in the brain would be particularly useful in the study of neuropsychiatric disorders in combination with a large-scale genome-wide association study. Using Wellcome Trust Case Control Consortium association study data, we identified SNPs associated with bipolar disorder and gene expression variation in the human brain. We found that SNPs in the *AKAP10* and *PRKCI* genes are significantly associated with bipolar disorder and gene expression variation.

1. Introduction

Identifying the genetic basis of gene expression variation in the human brain is important for understanding brain physiology and pathophysiology at the molecular level. Taking advantage of high-throughput genomic technologies, such as DNA microarrays, previous studies revealed that genetic variation plays a central role in the regulation of gene expression (Cheung et al., 2005; Dixon et al., 2007; Goring et al., 2007; Myers et al., 2007; Spielman et al., 2007; Stranger et al., 2005, 2007a,b). Most of these studies, however, used lymphoblastoid cells or lymphocytes, and only a few focused on human brain tissue (Liu et al., 2010; Myers et al., 2007). Given that genome-wide gene expression patterns vary considerably in human tissue (Shyamsundar et al., 2005), the effect of genetic variations was also expected to be different between lymphoblastoid cells and brain. We investigated the genetic basis of gene expression variation in human prefrontal cortex.

Knowledge of genetic variations contributing to differences in gene expression in the brain would be particularly useful in the study of neuropsychiatric diseases in combination with a large-scale genome-wide association study (GWAS). As an example, using GWAS data for bipolar disorder (The Wellcome Trust Case Control Consortium, 2007), we tried to identify the single nucleotide polymorphisms (SNPs) significantly associated with bipolar disorder and gene expression variation in the human brain.

2. Materials and methods

2.1. Postmortem brain, DNA extraction, and SNP array

Fresh-frozen postmortem prefrontal cortices (Brodmann's area 46, $n = 105$) were obtained from the Stanley Medical Research Institute (SMRI). Genomic DNA was extracted as previously described (Iwamoto et al., 2007). Genotyping was performed with the Affymetrix GeneChip Human Mapping 500K Array Set according to the manufacturer's standard protocols (Affymetrix, Santa Clara, CA, USA), with minor modifications. Briefly, genomic DNA was digested with restriction endonuclease, ligated to an adaptor, and subjected to PCR amplification with adaptor-specific primers. The PCR products were digested with DNase I and labeled with a biotinylated nucleotide analogue using terminal

* Corresponding author at: Department of Molecular Psychiatry, Graduate School of Medicine, The University of Tokyo, 7-3-1 Hongo, Bunkyo-ku, Tokyo 351-0198, Japan. Tel.: +81 3 5800 9165; fax: +81 3 5800 9165.
** Corresponding author.
E-mail addresses: kaziwamoto-tky@umin.ac.jp (K. Iwamoto), kato@brain.riken.jp (T. Kato).

0168-0102/$ – see front matter. Crown Copyright © 2011 Published by Elsevier Ireland Ltd and the Japan Neuroscience Society. All rights reserved.
doi:10.1016/j.neures.2011.02.012

Table 1
Summary of study sample data.

	Study samples[a]	Control samples[b]
n	73	29
Diagnosis	29CT, 20BD, 24SZ	29CT
Sex (male:female)	47:26	23:6
Age (yrs)	44.3 ± 8.5	44.6 ± 7.7
Sample pH	6.65 ± 0.16	6.69 ± 0.17
Postmortem interval (h)	34.4 ± 15.8	30.2 ± 12.5
Side of brain (left:right)	43:30	14:15

CT, control; BD, bipolar disorder; SZ, schizophrenia.
[a] Expression profiles of study samples with high pH (pH ≥ 6.4).
[b] Expression profiles of control samples with high pH (pH ≥ 6.4).

deoxynucleotidyl transferase. The labeled DNA fragments were injected into the microarray cartridge equilibrated to hybridization temperature and hybridized to the microarray. The hybridized DNA probes were captured by streptavidin–phycoerythrin conjugates, and the arrays were scanned. All microarray data were deposited and are available through the SMRI Online Genomics Database (https://www.stanleygenomics.org). The present study was approved by the ethics committees of RIKEN.

2.2. Gene expression analysis and genotype analysis

In a previous study, we obtained gene expression profiles from the same prefrontal cortex samples as those used in the current study, using an Affymetrix U133A chip (Iwamoto et al., 2005). Among them, we used microarray data sets from subjects with high brain pH (pH ≥ 6.4, $n = 73$) in this study to avoid the effect of agonal factors (Iwamoto and Kato, 2006; Li et al., 2004; Tomita et al., 2004) (see Section 4 for details). Statistics for the sample sets used in this study are summarized in Table 1. The DNA microarray raw data were processed by MAS5 (Affymetrix) and imported into GeneSpring 7.1 software (Silicon Genetics, Redwood City, CA, USA). Data normalization was performed by dividing each microarray data set by its median value. Among the probes on the U133A array, we used 11,920 probes that showed the present or marginal call in more than half the samples. In genotyping analysis, allele calls were determined using the DM algorithm implemented in Affymetrix GeneChip Genotyping Analysis software. We used SNPs showing minor allele frequency ≥5%. Copy number (CN) state was determined using CNAT4.1 software (Affymetrix). A data set from male control subjects used in this study was employed for reference. In analyzing a male control subject, we used the rest of the control males for reference. Median normalization and a genomic smoothing size of 0.1 Mb were used.

2.3. Data analysis

Physical positions and annotations of SNPs, transcripts, and expression probes were obtained through the University of California Santa Cruz Genome Browser (http://genome.ucsc.edu) based on Genome Build 36 and the Affymetrix NetAffx database (http://www.affymetrix.com). Spearman's correlation was calculated using R software. For calculation of Spearman's correlation, each SNP genotype was converted to 1 (homozygous for one allele), 2 (heterozygous), or 3 (homozygous for the other allele). False discovery rate analysis was performed using QVALUE software (Storey and Tibshirani, 2003) implemented in R (http://www.bioconductor.org). For the comparison of *cis*-regulated transcripts with data from previous studies (Dixon et al., 2007; Goring et al., 2007; Stranger et al., 2007a), the gene list that appeared in the previous report was extracted. In the study by Stranger et al. (2007a), 323 transcripts identified in the CEU population (Utah, USA, residents of northern and western European origin)

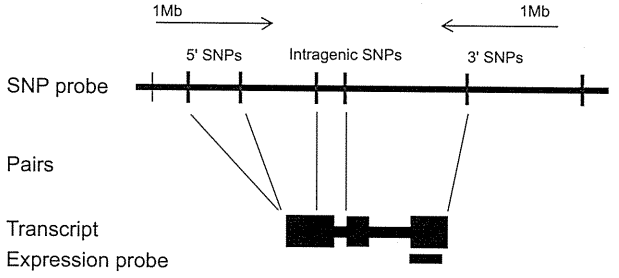

Fig. 1. Schematic representation of the relationship between single nucleotide polymorphism (SNP) and gene expression in this study. The genes that lie within 1 Mb upstream or downstream of a SNP were considered, and SNP-expression probe pairs were made for data analysis. The start and end positions of each gene were based on public ID obtained by the NetAffx database. In this example, five pairs were made for SNP analysis.

of the HapMap project (International Hapmap Consortium, 2005) were used for comparison. In the research by Dixon et al. (2007) and Goring et al. (2007), the same number of top-listing transcripts in this study ($n = 187$; Table 2) was selected for comparison. The qRT-PCR data were analyzed by Spearman's correlation.

2.4. Quantitative real-time RT-PCR

For qRT-PCR, 3 μg of total RNA was used for cDNA synthesis by oligo(dT) and SuperScript II reverse transcriptase (Invitrogen). qRT-PCR using the TaqMan PreAmp Master Mix Kit (Applied Biosystems, Foster City, CA, USA) was performed with the ABI PRISM 7900HT (Applied Biosystems). We performed 10 cycles of preamplification PCR using cDNA template and pooled TaqMan probes. After a 1:5 dilution of preamplified products, qRT-PCR using each TaqMan probe was performed according to the manufacturer's protocol (Applied Biosystems). Pooled TaqMan probes included ABI gene expression assay probes of *AKAP10* (Hs00895871_m1), *PRKCI* (Hs00995848_g1), *GAPDH* (Hs99999903_m1), and *ACTB* (Hs99999905_m1). The comparative Ct method was employed for quantification of transcripts according to the manufacturer's guidelines (Applied Biosystems).

3. Results

3.1. Analysis of cis-regulated transcripts

Using the postmortem brain samples, we had previously performed gene expression analysis using Affymetrix U133A chips (Iwamoto et al., 2005). From the probe sets (referred to here as probes and considered as transcripts) on the array, we used expression data for 11,920 brain-expressed probes. To consider the effect of agonal factors, which are the most severe confounding factors in gene expression in the human brain and which are related to sample pH (Iwamoto and Kato, 2006; Li et al., 2004; Tomita et al., 2004), we used data from high-pH samples (pH ≥ 6.4, $n = 73$) for analysis (Table 1).

Using standard protocols with minor modifications, we consistently obtained a high call rate (average call rate was 99.08% with the DM algorithm) in the genotype analysis. Of about 500,000 SNPs on the arrays, we used 381,812 SNPs that showed a minor allele frequency of ≥5% for assessing the effect of genetic variations using SNPs. In accordance with previous studies (Stranger et al., 2005, 2007a), we considered genes found within 1 Mb upstream or downstream of a SNP, and we made 3,072,984 pairs of expression and SNP probes for calculation of correlation (Fig. 1 and Table 2). Given that the *trans* effect is difficult to reproduce across studies (Dixon et al., 2007; Goring et al., 2007), we focused on the *cis* effect of

Please cite this article in press as: Iwamoto, K., et al., Survey of the effect of genetic variations on gene expression in human prefrontal cortex and its application to genetics of psychiatric disorders. Neurosci. Res. (2011), doi:10.1016/j.neures.2011.02.012

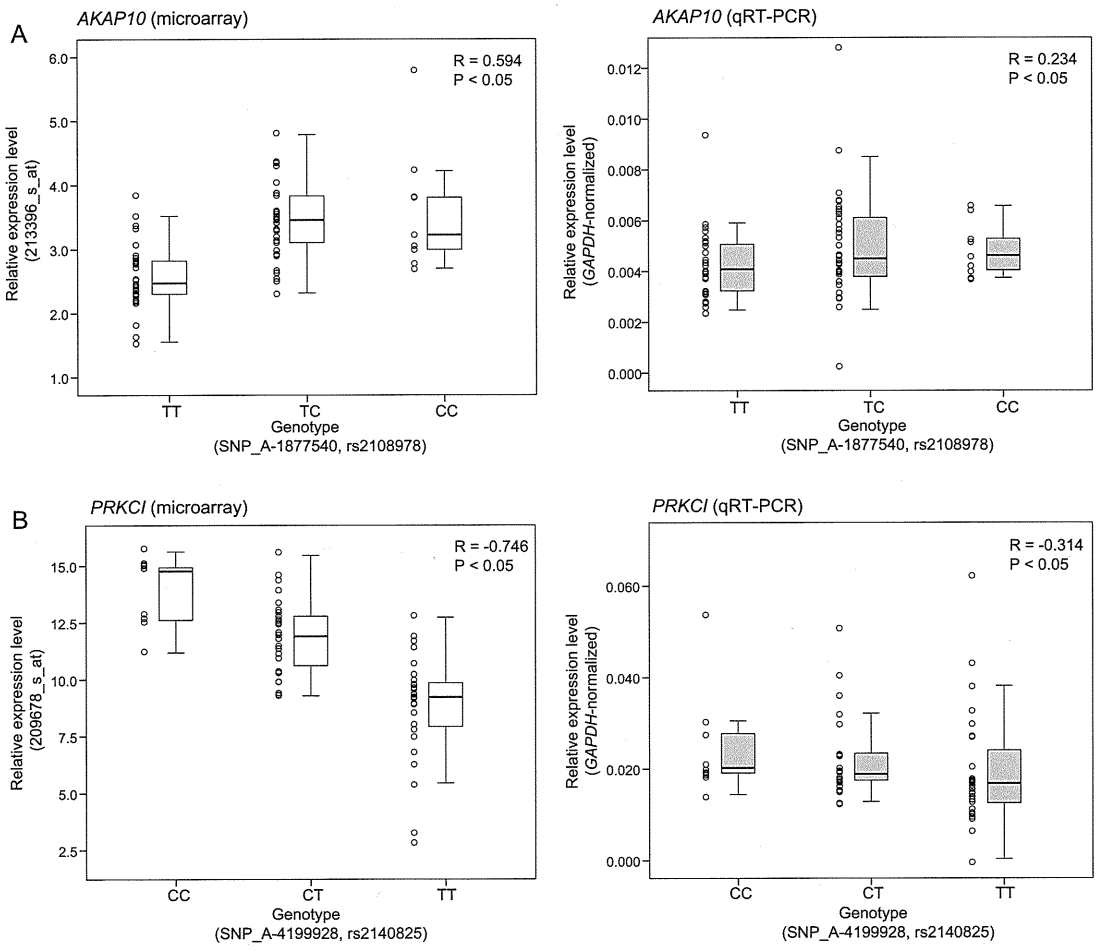

Fig. 2. SNP-expression correlation in *AKAP10* and *PRKCI* genes. Genetic variations in the (A) *AKAP10* (rs2108978) and (B) *PRKCI* (rs2140825) genes were correlated with their expression levels. The SNPs showing the highest significance in the Wellcome Trust Case Control Consortium bipolar disorder data were shown as representatives (Supplementary Tables 3 and 4). In both cases, the T allele is considered the risk allele.

genetic variations in this study. We used Spearman's rank correlation (Stranger et al., 2007b) and then applied a false discovery rate of <0.05 to correct for multiple testing. After that, we tested correlation using only high-pH control subjects ($n = 29$, Supplementary Table 1), to exclude the effect of diagnosis- or patient-related confounding factors. The resultant 1019 pairs included 187 expression and 872 SNP probes (Table 2, Supplementary Tables 1 and 2). Given the number of unique expression probes, we estimated that at least 1.6% of the transcripts are reliably *cis*-regulated in our sample set. Consistent with a previous report (Stranger et al., 2007a), strong correlations tended to be restricted to distances of 100 kb (Supplementary Fig. 1).

Gene ontology (http://www.geneontology.org) analysis of the obtained transcripts using the Database for Annotation, Visualization and Integrated Discovery (DAVID) (Dennis et al., 2003) or GeneSpring software revealed that some categories were over-represented with weak significance, but none of the categories showed strong significance after multiple-testing correction (data not shown). These results suggest that the *cis*-regulated transcripts were distributed over a wide range of biological functions in human brain.

Table 2
Summary of analysis of *cis*-regulated transcripts using genotype information.

	Pairs	SNP probe[a]	Expression probe[a]
n	3,072,984	349,400	11,785
$P<0.05$	169,117	108,663	11,473
FDR (0.05)	1099	945	205
$P<0.05$ in control[b]	1019	872	187

FDR, false discovery rate.
[a] Number of unique probes are listed.
[b] Significant pairs and transcripts are in Supplementary Tables 1 and 2, respectively.

We found that our list included the transcripts previously identified as *cis*-regulated in other studies using lymphoblastoid cells or lymphocytes. Comparing our data with data from the previous studies, we found that *POMZP3* (Cheung et al., 2005; Spielman et al., 2007), *CPNE1* (Cheung et al., 2005; Stranger et al., 2005), *RPS26* (Cheung et al., 2005), *PPAT* (Cheung et al., 2005), *PEX6* (Spielman et al., 2007), *DNAJC15* (Spielman et al., 2007), *HSD17B12* (Spielman et al., 2007), and *TPP2* (Spielman et al., 2007) were included in our list of 187 *cis*-regulated transcripts. When we compared *cis*-regulated transcripts with other studies that provided the genome-wide list, at least 11 (Goring et al., 2007), 17 (Stranger et al., 2007a), and 21 (Dixon et al., 2007) transcripts were found to be in common. These results suggest that 5.9–11.2% of *cis*-regulated transcripts in the brain are also conserved in lymphoblastoid cells or lymphocytes.

Among the identified significantly associated pairs in this study, some SNPs were mapped to copy number variable regions (CNVRs), as described below. They made a total of 101 pairs consisting of 69 SNP and 14 expression probes. When we reanalyzed data by

Please cite this article in press as: Iwamoto, K., et al., Survey of the effect of genetic variations on gene expression in human prefrontal cortex and its application to genetics of psychiatric disorders. Neurosci. Res. (2011), doi:10.1016/j.neures.2011.02.012

Spearman's correlation after removing subjects showing an altered CN state, all pairs still showed significance (Supplementary Table 1). Therefore, we concluded that the effect of an altered CN state was smaller than the effect of SNPs on expression of these genes.

3.2. Identifying SNPs associated with bipolar disorder and gene expression variation in the brain

When we compared the list of 872 SNPs identified in this study (Supplementary Table 1) with the results of the Wellcome Trust Case Control Consortium (WTCCC) association study of bipolar disorder (The Wellcome Trust Case Control Consortium, 2007), 29 SNPs around 9 genes were common in the additive model ($P < 0.05$) (Supplementary Table 3). After Bonferroni's correction was applied, 3 SNPs in the *AKAP10* gene showed significant association. Similarly, 43 SNPs around 18 genes were associated with bipolar disorder in the general model (Supplementary Table 4). We found that a SNP in the *PRKCI* gene showed significant association after application of Bonferroni's correction. We confirmed that expression levels of these genes are significantly correlated with genotype by qRT-PCR analysis (Fig. 2).

4. Discussion

Gene expression analysis in the human brain is challenging because of many uncontrollable factors (Atz et al., 2007; Iwamoto and Kato, 2006; Mirnics et al., 2006; Papapetropoulos et al., 2007; Ryan et al., 2004; Weis et al., 2007). Subjects with prolonged agonal states (terminal condition of death), such as respiratory failure or coma, tend to have decreased brain pH. Although the mechanism remains unclear, postmortem brains with low pH, compared with those with high pH, exhibit a distinctive gene expression pattern in a genome-wide manner (Bahn et al., 2001; Barton et al., 1993; Harrison et al., 1995; Kingsbury et al., 1995; Li et al., 2004; Tomita et al., 2004). Previously, we systematically assessed the effect of demographic variables (e.g., gender, side of brain, sample pH, postmortem interval, age, diagnosis, cause of death) on gene expression (Iwamoto et al., 2006). We confirmed that the most severe confounding factor was sample pH, affecting expression of about 30–50% of probes on the array (Iwamoto et al., 2006). Using samples with a pH $\geq$6.4 clearly reduced the effect of sample pH in our brain set (Iwamoto and Kato, 2006). Therefore, we used a sample pH of 6.4 as the threshold in our current study. Although the number of samples analyzed was decreased, identified *cis*-regulated transcripts were well consistent with those identified in previous studies. Moreover, these results suggested that *cis*-regulation of transcripts is substantially conserved across different tissues. However, more careful consideration would be needed for a precise estimation of this conservation, such as differences in sample size, analytical approach, and platform.

We examined the relationship between SNP and genotype within 1 Mb from a SNP in the current study. Because we observed that strong correlation was restricted to distances of about 100 kb, our analysis covered enough range to detect the correlations. It will be interesting to examine the long-range *cis* effect, as well as the *trans* effect. However, because such analysis has been reported to be difficult to reproduce across studies (Dixon et al., 2007; Goring et al., 2007), we focused on the *cis* effect of genetic variations in this study.

Myers et al. (2007) first reported *cis*-regulated transcripts in the human brain using SNP information. When we compared *cis*-regulated transcripts, we obtained 14 *cis*-regulated transcripts in common (7.5%). Given that the previous study used very old brains (average age, 81 years; range, 65–100 years) and different regions of these brains (Myers et al., 2007), differences in sample age might be one reason for the modest concordance. Although we could not rule out the effect of using a different platform for expression profiling, these results suggest that genetic effects of gene expression in the human brain differ by brain region and developmental stage. In contrast, we found that our results are in good agreement with results obtained by Liu et al. (2010). Among the 119 top-scored SNP-expression pairs reported, 40 pairs (33.6%) were confirmed in our study. Compared with our study, Liu et al. (2010) used the same sample source and platform but a different analytical approach. Most importantly, they also considered brain pH as a covariate. The concordance of these two studies further supports the importance of brain pH as a confounding factor in genotype-expression analysis.

Our results as well as others may have been influenced by the presence of genetic variations such as SNPs and CNVRs located in the probe sets. Indeed, we estimated that 39.2% of probe sets used in the expression microarray contain at least one SNP (data not shown). In such a situation, the precise effect of genetic variations should be determined only by the sequencing analyses around probe regions in all analyzed samples. Alternatively, utilizing next-generation sequencing technologies will greatly improve this problem.

Sixty-eight percent of the 187 expression probes showed significant correlation with multiple SNPs. In addition, most of them (84%) showed that multiple SNPs are in linkage disequilibrium. Although the effect of linkage disequilibrium would be taken into account in data analysis such as multiple-testing correction, the presence of multiple SNPs would further support the association with expression.

Knowledge of genetic variations contributing to differences in gene expression in the brain would be particularly useful in the study of neuropsychiatric diseases in combination with a large-scale GWAS. By comparing the list of SNPs associated with bipolar disorder in the WTCCC study (The Wellcome Trust Case Control Consortium, 2007), we found that SNPs in the *AKAP10* and *PRKCI* genes were in common after multiple-testing correction. Although the function of *PRKCI* in the brain is not known, a role for protein kinase C in the pathophysiology of bipolar disorder has been suggested (Hahn and Friedman, 1999). Multiple lines of evidence suggest that *AKAP10* may also play a role in bipolar disorder. *AKAP10* encodes an anchoring protein that interacts with the regulatory subunit of protein kinase A (PKA) (Wang et al., 2001). A genome-wide search for aging-related genes found that a non-synonymous SNP of *AKAP10*, I646V (rs203462), which inhibits binding to PKA, is significantly less frequently seen in older healthy subjects compared with younger subjects, suggesting that this SNP is associated with disease susceptibility (Kammerer et al., 2003). Although the function of *AKAP10* is not yet entirely elucidated, AKAP10 protein has RGS (regulator of G-protein signaling) domains and is localized to mitochondria (Burns-Hamuro et al., 2004). Because both Gs-cAMP-PKA signaling (Chang et al., 2003) and mitochondrial dysfunction (Kato, 2008) have been implicated in bipolar disorder, altered expression of *AKAP10* might affect the pathophysiology of bipolar disorder through these pathways.

In summary, we investigated the genetic basis of gene expression variation in human prefrontal cortex using both SNP and gene expression information. By comparing the WTCCC study's list of SNPs associated with bipolar disorder, we found that SNPs in the *AKAP10* and *PRKCI* genes are significantly associated with bipolar disorder and gene expression variation in the human brain. Our data set will aid the search for candidate genes in functional studies of neuropsychiatric disorders.

Acknowledgments

This study was supported by Grant-in-Aid for Young Scientists and for Scientific Research on Innovative Areas (Comprehensive

Please cite this article in press as: Iwamoto, K., et al., Survey of the effect of genetic variations on gene expression in human prefrontal cortex and its application to genetics of psychiatric disorders. Neurosci. Res. (2011), doi:10.1016/j.neures.2011.02.012

Brain Science Network) from the Ministry of Education, Science, Sports and Culture of Japan. Postmortem brain samples were donated by the Stanley Medical Research Institute, courtesy of Drs. Michael B. Knable, E. Fuller Torrey, Maree J. Webster, and Robert H. Yolken. We thank Y. Nakano and A. Nishida for their technical assistances. This study makes use of data generated by the Wellcome Trust Case Control Consortium. A full list of the investigators who contributed to the generation of the data is available from www.wtccc.org.uk. Funding for the project was provided by the Wellcome Trust under award 076113.

Appendix A. Supplementary data

Supplementary data associated with this article can be found, in the online version, at doi:10.1016/j.neures.2011.02.012.

References

Atz, M., Walsh, D., Cartagena, P., Li, J., Evans, S., Choudary, P., Overman, K., Stein, R., Tomita, H., Potkin, S., Myers, R., Watson, S.J., Jones, E.G., Akil, H., Bunney Jr., W.E., Vawter, M.P., 2007. Methodological considerations for gene expression profiling of human brain. J. Neurosci. Methods 163, 295–309.

Bahn, S., Augood, S.J., Ryan, M., Standaert, D.G., Starkey, M., Emson, P.C., 2001. Gene expression profiling in the post-mortem human brain – no cause for dismay. J. Chem. Neuroanat. 22, 79–94.

Barton, A.J., Pearson, R.C., Najlerahim, A., Harrison, P.J., 1993. Pre- and postmortem influences on brain RNA. J. Neurochem. 61, 1–11.

Burns-Hamuro, L.L., Barraclough, D.M., Taylor, S.S., 2004. Identification and functional analysis of dual-specific A kinase-anchoring protein-2. Methods Enzymol. 390, 354–374.

Chang, A., Li, P.P., Warsh, J.J., 2003. Altered cAMP-dependent protein kinase subunit immunolabeling in post-mortem brain from patients with bipolar affective disorder. J. Neurochem. 84, 781–791.

Cheung, V.G., Spielman, R.S., Ewens, K.G., Weber, T.M., Morley, M., Burdick, J.T., 2005. Mapping determinants of human gene expression by regional and genome-wide association. Nature 437, 1365–1369.

Dennis Jr., G., Sherman, B.T., Hosack, D.A., Yang, J., Gao, W., Lane, H.C., Lempicki, R.A., 2003. DAVID: database for annotation, visualization, and integrated discovery. Genome Biol. 4, P3.

Dixon, A.L., Liang, L., Moffatt, M.F., Chen, W., Heath, S., Wong, K.C., Taylor, J., Burnett, E., Gut, I., Farrall, M., Lathrop, G.M., Abecasis, G.R., Cookson, W.O., 2007. A genome-wide association study of global gene expression. Nat. Genet. 39, 1202–1207.

Goring, H.H., Curran, J.E., Johnson, M.P., Dyer, T.D., Charlesworth, J., Cole, S.A., Jowett, J.B., Abraham, L.J., Rainwater, D.L., Comuzzie, A.G., Mahaney, M.C., Almasy, L., MacCluer, J.W., Kissebah, A.H., Collier, G.R., Moses, E.K., Blangero, J., 2007. Discovery of expression QTLs using large-scale transcriptional profiling in human lymphocytes. Nat. Genet. 39, 1208–1216.

Hahn, C.G., Friedman, E., 1999. Abnormalities in protein kinase C signaling and the pathophysiology of bipolar disorder. Bipolar Disord. 1, 81–86.

Harrison, P.J., Heath, P.R., Eastwood, S.L., Burnet, P.W., McDonald, B., Pearson, R.C., 1995. The relative importance of premortem acidosis and postmortem interval for human brain gene expression studies: selective mRNA vulnerability and comparison with their encoded proteins. Neurosci. Lett. 200, 151–154.

International Hapmap Consortium, 2005. A haplotype map of the human genome. Nature 437, 1299–1320.

Iwamoto, K., Bundo, M., Kato, T., 2005. Altered expression of mitochondria-related genes in postmortem brains of patients with bipolar disorder or schizophrenia, as revealed by large-scale DNA microarray analysis. Hum. Mol. Genet. 14, 241–253.

Iwamoto, K., Bundo, M., Ueda, J., Kato, T., 2006. Expression of ribosomal subunit genes increased coordinately with postmortem interval in human brain. Mol. Psychiatry 11, 1067–1069.

Iwamoto, K., Kato, T., 2006. Gene expression profiling in schizophrenia and related mental disorders. Neuroscientist 12, 349–361.

Iwamoto, K., Ueda, J., Nakano, Y., Bundo, M., Ukai, W., Hashimoto, E., Saito, T., Kato, T., 2007. Evaluation of whole genome amplification methods using postmortem brain samples. J. Neurosci. Methods 165, 104–110.

Kammerer, S., Burns-Hamuro, L.L., Ma, Y., Hamon, S.C., Canaves, J.M., Shi, M.M., Nelson, M.R., Sing, C.F., Cantor, C.R., Taylor, S.S., Braun, A., 2003. Amino acid variant in the kinase binding domain of dual-specific A kinase-anchoring protein 2: a disease susceptibility polymorphism. Proc. Natl. Acad. Sci. U.S.A. 100, 4066–4071.

Kato, T., 2008. Molecular neurobiology of bipolar disorder: a disease of 'mood-stabilizing neurons'? Trends Neurosci. 31, 495–503.

Kingsbury, A.E., Foster, O.J., Nisbet, A.P., Cairns, N., Bray, L., Eve, D.J., Lees, A.J., Marsden, C.D., 1995. Tissue pH as an indicator of mRNA preservation in human post-mortem brain. Brain Res. Mol. Brain Res. 28, 311–318.

Li, J.Z., Vawter, M.P., Walsh, D.M., Tomita, H., Evans, S.J., Choudary, P.V., Lopez, J.F., Avelar, A., Shokoohi, V., Chung, T., Mesarwi, O., Jones, E.G., Watson, S.J., Akil, H., Bunney Jr., W.E., Myers, R.M., 2004. Systematic changes in gene expression in postmortem human brains associated with tissue pH and terminal medical conditions. Hum. Mol. Genet. 13, 609–616.

Liu, C., Cheng, L., Badner, J.A., Zhang, D., Craig, D.W., Redman, M., Gershon, E.S., 2010. Whole-genome association mapping of gene expression in the human prefrontal cortex. Mol. Psychiatry 15, 779–784.

Mirnics, K., Levitt, P., Lewis, D.A., 2006. Critical appraisal of DNA microarrays in psychiatric genomics. Biol. Psychiatry 60, 163–176.

Myers, A.J., Gibbs, J.R., Webster, J.A., Rohrer, K., Zhao, A., Marlowe, L., Kaleem, M., Leung, D., Bryden, L., Nath, P., Zismann, V.L., Joshipura, K., Huentelman, M.J., Hu-Lince, D., Coon, K.D., Craig, D.W., Pearson, J.V., Holmans, P., Heward, C.B., Reiman, E.M., Stephan, D., Hardy, J., 2007. A survey of genetic human cortical gene expression. Nat. Genet. 39, 1494–1499.

Papapetropoulos, S., Shehadeh, L., McCorquodale, D., 2007. Optimizing human post-mortem brain tissue gene expression profiling in Parkinson's disease and other neurodegenerative disorders: from target "fishing" to translational breakthroughs. J. Neurosci. Res. 85, 3013–3024.

Ryan, M.M., Huffaker, S.J., Webster, M.J., Wayland, M., Freeman, T., Bahn, S., 2004. Application and optimization of microarray technologies for human post-mortem brain studies. Biol. Psychiatry 55, 329–336.

Shyamsundar, R., Kim, Y.H., Higgins, J.P., Montgomery, K., Jorden, M., Sethuraman, A., van de Rijn, M., Botstein, D., Brown, P.O., Pollack, J.R., 2005. A DNA microarray survey of gene expression in normal human tissues. Genome Biol. 6, R22.

Spielman, R.S., Bastone, L.A., Burdick, J.T., Morley, M., Ewens, W.J., Cheung, V.G., 2007. Common genetic variants account for differences in gene expression among ethnic groups. Nat. Genet. 39, 226–231.

Storey, J.D., Tibshirani, R., 2003. Statistical significance for genomewide studies. Proc. Natl. Acad. Sci. U.S.A. 100, 9440–9445.

Stranger, B.E., Forrest, M.S., Clark, A.G., Minichiello, M.J., Deutsch, S., Lyle, R., Hunt, S., Kahl, B., Antonarakis, S.E., Tavare, S., Deloukas, P., Dermitzakis, E.T., 2005. Genome-wide associations of gene expression variation in humans. PLoS Genet. 1, e78.

Stranger, B.E., Forrest, M.S., Dunning, M., Ingle, C.E., Beazley, C., Thorne, N., Redon, R., Bird, C.P., de Grassi, A., Lee, C., Tyler-Smith, C., Carter, N., Scherer, S.W., Tavare, S., Deloukas, P., Hurles, M.E., Dermitzakis, E.T., 2007a. Relative impact of nucleotide and copy number variation on gene expression phenotypes. Science 315, 848–853.

Stranger, B.E., Nica, A.C., Forrest, M.S., Dimas, A., Bird, C.P., Beazley, C., Ingle, C.E., Dunning, M., Flicek, P., Koller, D., Montgomery, S., Tavare, S., Deloukas, P., Dermitzakis, E.T., 2007b. Population genomics of human gene expression. Nat. Genet. 39, 1217–1224.

The Wellcome Trust Case Control Consortium, 2007. Genome-wide association study of 14,000 cases of seven common diseases and 3000 shared controls. Nature 447, 661–678.

Tomita, H., Vawter, M.P., Walsh, D.M., Evans, S.J., Choudary, P.V., Li, J., Overman, K.M., Atz, M.E., Myers, R.M., Jones, E.G., Watson, S.J., Akil, H., Bunney Jr., W.E., 2004. Effect of agonal and postmortem factors on gene expression profile: quality control in microarray analyses of postmortem human brain. Biol. Psychiatry 55, 346–352.

Wang, L., Sunahara, R.K., Krumins, A., Perkins, G., Crochiere, M.L., Mackey, M., Bell, S., Ellisman, M.H., Taylor, S.S., 2001. Cloning and mitochondrial localization of full-length D-AKAP2, a protein kinase A anchoring protein. Proc. Natl. Acad. Sci. U.S.A. 98, 3220–3225.

Weis, S., Llenos, I.C., Dulay, J.R., Elashoff, M., Martinez-Murillo, F., Miller, C.L., 2007. Quality control for microarray analysis of human brain samples: the impact of postmortem factors, RNA characteristics, and histopathology. J. Neurosci. Methods 165, 198–209.

Please cite this article in press as: Iwamoto, K., et al., Survey of the effect of genetic variations on gene expression in human prefrontal cortex and its application to genetics of psychiatric disorders. Neurosci. Res. (2011), doi:10.1016/j.neures.2011.02.012

Epigenetics 6:4; 508-515; April 2011; © 2011 Landes Bioscience

Comprehensive DNA methylation analysis of human peripheral blood leukocytes and lymphoblastoid cell lines

Hiroko Sugawara,[1,2] Kazuya Iwamoto,[3] Miki Bundo,[3] Junko Ueda,[1] Jun Ishigooka[2] and Tadafumi Kato[1,*]

[1]Laboratory for Molecular Dynamics of Mental Disorders; RIKEN Brain Science Institute; Saitama, Japan; [2]Department of Psychiatry; Tokyo Women's Medical University; [3]Department of Molecular Psychiatry; Graduate School of Medicine; The University of Tokyo; Tokyo, Japan

Key words: DNA methylation, lymphoblastoid cell lines, peripheral blood leukocytes, LUMA, promoter tiling array, gene expression

DNA methylation is involved in development and in human diseases. Genomic DNA derived from lymphoblastoid cell lines (LCLs) is commonly used to study DNA methylation. There are potential confounding factors regarding the use of LCL-derived DNA, however, such as Epstein-Barr (EB) viral infection and artifacts induced during cell culture. Recently, several groups compared the DNA methylation status of peripheral blood leukocytes (PBLs) and LCLs and concluded that the DNA methylation profiles between them might be consistent. To confirm and extend theses results, we performed a comprehensive DNA methylation analysis using both PBLs and LCLs derived from the same individuals. Using the luminometric methylation assay, we revealed that the global DNA methylation level was different between PBLs and LCLs. Furthermore, the direction of change was not consistent. Comparisons of genome-wide DNA methylation patterns of promoter regions revealed that methylation profiles were largely conserved between PBLs and LCLs. A preliminary analysis in a small number of samples suggested that the methylation status of an LCL may be better correlated with PBLs from the same individual than with LCLs from other individuals. Expectedly, DNA methylation in promoter regions overlapping with CpG islands was associated with gene silencing in both PBLs and LCLs. With regard to methylation differences, we found that hypermethylation was more predominant than hypomethylation in LCLs compared with PBLs. These findings suggest that LCLs should be used for DNA methylation studies with caution as the methylation patterns of promoter regions in LCLs are not always the same as those in PBLs.

Introduction

In medical genetics, the main sources of genomic DNA are peripheral blood leukocytes (PBLs) and Epstein-Barr (EB) virus-transformed lymphoblastoid cell lines (LCLs). LCLs have a great advantage in that they provide an unlimited source of DNA, though some studies report that LCLs are susceptible to genomic instability.[1-4]

In addition to DNA variations and mutations, DNA modifications are an important factor in disease development and progression.[5] DNA methylation at the cytosine residue of the CpG site, the main DNA modification in mammals, is involved in gene silencing, tissue differentiation, genomic imprinting and X chromosome inactivation. Aberrant DNA methylation is related to various diseases and developmental disabilities such as cancer and mental retardation.[6]

Genomic DNA derived from LCLs is most useful for studying DNA methylation, because studying DNA methylation generally requires a large amount of DNA. LCLs are not a simple alternative for PBLs, however, because LCLs comprise infected B lymphocytes, whereas PBLs contain various types of blood cells. In addition, several factors potentially affect DNA methylation patterns in LCLs compared to the original B lymphocytes, including EB virus infection, immortalization, cell culture conditions and freezing cycles. Grafodatskaya et al. reported that methylation alterations in LCLs are more profound in highly passaged cells, but freezing cells that have been passaged only a few times does not significantly affect DNA methylation.

Here, we performed a comprehensive DNA methylation analysis using both PBLs and LCL genomic DNA derived from the same individuals to identify the altered methylation patterns in LCLs. The goal of this study was to determine the utility of LCLs for DNA methylation analysis associated with human diseases. In previous studies, Brennan et al. compared DNA methylation profiles in the promoter regions of a subset of genes, and Grafodatskaya et al. and Sun et al. compared genome-wide CpG site DNA methylation by obtaining snapshots or signatures of samples.

To our knowledge, however, there are no comprehensive DNA methylation analyses that focused on whole genome promoter

*Correspondence to: Tadafumi Kato; Email: kato@brain.riken.jp
Submitted: 07/12/10; Accepted: 01/19/11
DOI: 10.4161/epi.6.4.14876

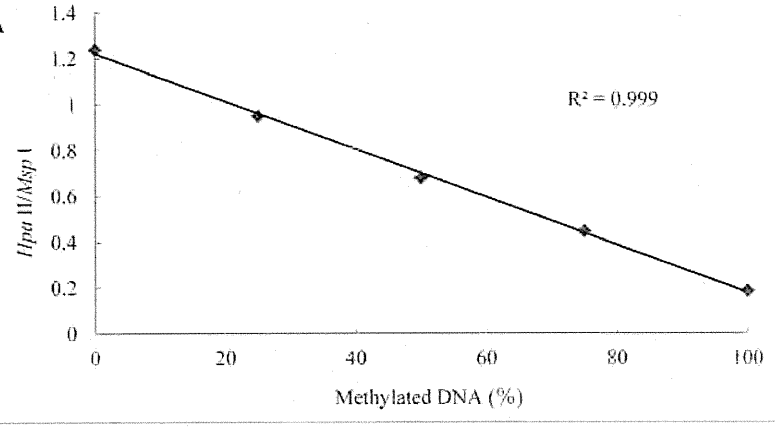

B

Subject	Age	Sex	*Hpa* II/*Msp* I		Direction of alteration
			PBL	LCL	
C1	29	M	0.57	0.21	↓
C3	25	F	0.35	0.44	↑
C4	52	M	0.32	0.52	↑

Figure 1. Global DNA methylation analysis using luminometric methylation assay (LUMA). (A) The linearity of the LUMA, assessed using standard DNA samples. Unmethylated DNA generated by whole genome amplification, as well as methylated DNA generated by treating the unmethylated DNA with SssI methylase were mixed in different proportions to obtain samples with 0, 25, 50, 75 or 100% methylated DNA. (B) Methylation levels of three sets of PBLs and LCLs derived from the same individual. All LCLs were low-passage without freezing.

regions using an ample number of samples. In the present study, we first compared global DNA methylation levels with three sets of PBLs and LCLs using a luminometric methylation assay (LUMA).[10,11] We then performed a promoter tiling array analysis to compare genome-wide DNA methylation patterns of promoter regions between four sets of PBLs and LCLs.

Results

Global DNA methylation levels between PBLs and LCLs. We examined the global DNA methylation levels of three sets of PBLs and LCLs by the LUMA method. All LCLs were low-passage without freezing. The accuracy and linearity of this assay were verified by inclusion of standard samples containing different proportions of methylated DNA. An inverse correlation between the CpG methylation level and the *Hpa*II/*Msp*I ratio was observed (R^2 = 0.999, **Fig. 1A**), demonstrating the applicability of the assay to detect subtle changes in DNA methylation in our experiments. The LUMA revealed alterations of *Hpa*II/*Msp*I ratios ranging from 0.57–0.21 (C1), 0.35–0.44 (C3) and 0.32–0.52 (C4), demonstrating a difference in the global DNA methylation level between PBLs and LCLs and the direction of the change was not consistent (**Fig. 1B**).

Comparison of genome-wide promoter methylation patterns between PBLs and LCLs. We examined the genome-wide promoter methylation patterns of four sets of PBLs and LCLs. Correlation coefficients (R) of the signal intensity of all probes between any two samples are shown in **Figure 2**. The average R value among PBLs and LCLs was 0.85 and 0.69, respectively, and there was a significant difference between them (p value = 0.007, unpaired t-test; **Fig. 2B**). Among the sets of PBLs and LCLs from the same individuals, the mean R value was 0.77. This was not significantly different from the R values among PBLs (p value = 0.125, unpaired t-test). The methylation pattern in LCLs of an individual tended to be more similar to that of their own PBLs than to the LCLs of others (**Sup. Fig. 1**), although the number of samples is too small to draw a conclusion.

Features of methylated regions in PBLs (PBL MRs) and LCLs (LCL MRs). We detected methylated regions (MRs) in PBLs and LCLs using MAT software,[12] and extracted 1,510 regions as PBL MRs and 2,587 regions as LCL MRs (**Table 1**). The common MRs between PBL MRs and LCL MRs comprised 1,379 regions, indicating that the methylation profiles were largely conserved between PBLs and LCLs. In addition, through rigorous data analysis, we detected specifically methylated regions in the PBLs (PBL-specific MRs; **Sup. Table 1**) and LCLs (LCL-specific MRs; **Sup. Table 2**). We performed bisulfite sequencing to validate the results of tiling array. The methylation patterns in each candidate region of PBL-specific MRs and LCL-specific MRs were confirmed using the samples used for tiling array (**Sup. Fig. 2**). The number of LCL-specific MRs was about eight times greater than that of PBL-specific MRs (**Table 1**). The number of genes located within 3 kb of the MRs is summarized in Table 1.

Ontology analysis of the methylation-associated genes. We performed a PANTHER ontology analysis using the gene lists of the PBL MRs and LCL MRs (**Table 2**). It seems that genes related to LCL MRs are more diverse compared with those related to PBL MRs (**Table 2**). However, when we closely examined the ontologies enriched in the genes related to LCL-specific MRs, most of the ontologies enriched in the LCL-specific MRs were included in those enriched in PBL MRs (**Sup. Table 3**). This is paradoxical; however, it would be reasonable to ascribe the apparently large number ontologies enriched in LCL MRs to the large number of genes within 3 kb of LCL MRs (N = 1,477) compared with PBL MRs (N = 768).

Correlation between DNA methylation and gene expression. Methylation of the CpG islands in promoter regions contributes to silencing gene expression.[13] Using the GEO database, we retrieved gene expression datasets for the PBLs (GSE6613, N = 22 controls[14] and GSE10041, N = 23 controls[15]), and LCLs (GSE12408, N = 17 controls[16] and GSE13122, N = 13 controls[17]), derived from control subjects. We selected the probe sets whose

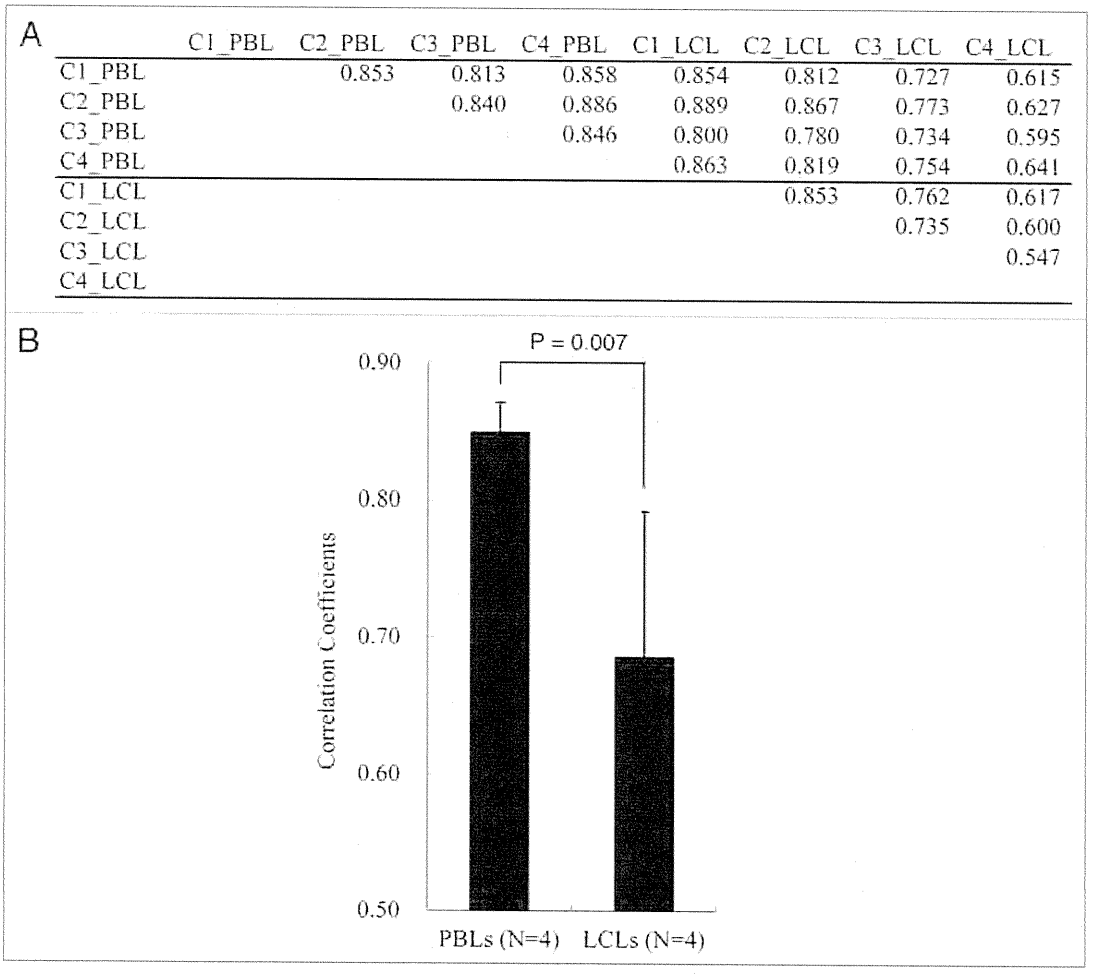

Figure 2. Correlation coefficients. (A) Correlation coefficients between all pair-wise comparisons. (B) Comparison of average correlation between PBLs or LCLs from four individuals. Student's t-test p value is given.

promoter regions were associated with the PBL MRs overlapping with CpG islands and examined their expression status based on flag analysis. In both datasets for PBLs, genes with promoters on PBL MRs were significantly more silenced in PBLs compared with all genes (p = 3.54E-03 for GSE6613 and 1.99E-03 for GSE10041; Fisher's exact test; **Fig. 3A and B**). Similarly, the genes with promoters on LCL MRs were significantly more silenced in LCLs compared with all genes (p = 2.98E-03 for GSE12408 and p = 4.10E-05 for GSE13122; **Fig. 4A and B**). These results are consistent with current knowledge that DNA methylation of CpG islands in promoter regions is relevant to gene silencing.

Individual alteration of DNA methylation pattern in LCLs. We then analyzed the methylated regions in individual subjects and detected specific methylated regions in the PBLs or LCLs in each of the four subjects separately (**Table 3**). The number of LCL-specific MRs was greater than that of PBL-specific MRs in three of the four sets, consistent with the finding of a previous study in reference 7. However, we also observed the opposite case (C4), suggesting that the direction of the methylation changes is possibly stochastic at the cell line level. The fact that there was few number of MRs overlapping among all four cell lines is consistent with this possibility.

Table 1. Summary of number of MRs and genes located within 3 kb from MRs

Category of MRs	Number of MRs	Number of associated genes
PBL MRs	1510	768
LCL MRs	2587	1477
common MRs	1379	699
PBL-specific MRs	63	30
LCL-specific MRs	509	611

PBL, peripheral blood lymphocyte; LCL, lymphoblastoid cell line; MRs, methylated regions.

Discussion

LCLs are widely used for many aspects of genetic and epigenetic studies. In an individual, the DNA sequence is generally common to most cell types and is fixed through life. In contrast, the DNA methylation pattern changes during the course of development.

Table 2. Ontology analysis of the genes related to PBL MRs and LCL MRs

Term	Category	PBL_MRs (768 IDs)			LCL_MRs (1477 IDs)		
		Counts	Expected	p value	Counts	Expected	p value
Cadherin	MF	19	3.35	4.57E-07	47	6.45	7.18E-23
Cadherin signaling pathway	PA	21	5.07	1.45E-05	49	9.76	3.50E-17
Nucleoside, nucleotide and nucleic acid metabolism	BP	160	100.96	7.55E-08	313	194.16	3.04E-16
Wnt signaling pathway	PA	32	10.51	9.12E-06	69	20.21	1.22E-15
Cell adhesion molecule	MF	28	11.93	1.24E-03	65	22.94	8.77E-12
Cell adhesion-mediated signaling	BP	27	11.45	1.06E-02	58	22.01	1.77E-08
mRNA transcription	BP	92	57.8	1.27E-03	172	111.16	1.98E-06
Chromatin packaging and remodeling	BP	19	7.16	2.27E-02	39	13.76	2.36E-06
Transcription factor	MF	99	61.97	9.57E-05	177	119.18	3.70E-06
Zinc finger transcription factor	MF	53	27.21	7.94E-04	93	52.33	2.25E-05
Signal transduction	BP	139	102.86	4.43E-03	263	197.82	3.14E-05
Protein modification	BP	59	34.94	1.24E-02	108	67.2	2.27E-04
Cell communication	BP	59	36.63	4.17E-02	111	70.45	3.94E-04
Spermatogenesis and motility	BP	15	3.9	2.71E-03	23	7.49	7.43E-04
Cell motility	BP	25	10.63	1.52E-02	42	20.44	2.41E-03
Gametogenesis	BP	19	7.28	2.80E-02	30	14	1.80E-02
Cell adhesion	BP	33	18.78	ns	75	36.12	1.95E-07
Nucleic acid binding	MF	113	86.07	ns	239	165.52	1.71E-07
Single-stranded DNA-binding protein	MF	5	0.69	ns	8	1.34	1.23E-02
Cell structure and motility	BP	51	34.67	ns	98	66.67	4.20E-03
Transferase	MF	41	26.7	ns	85	51.34	2.06E-04
Cell cycle	BP	45	30.47	ns	85	58.6	1.70E-02
Protein metabolism and modification	BP	115	91.81	ns	223	176.56	5.53E-03
mRNA transcription regulation	BP	65	44.06	ns	122	84.74	9.88E-03
Miscellaneous	BP	10	4.23	ns	19	8.13	2.34E-02
Intracellular protein traffic	BP	42	30.44	ns	86	58.54	1.08E-02
Histone	MF	8	2.6	ns	15	4.99	3.49E-02
Developmental processes	BP	78	64.99	ns	167	124.99	3.06E-03
G-protein modulator	MF	20	12.23	ns	45	23.52	7.29E-03
Select regulatory molecule	MF	43	35.94	ns	99	69.11	8.77E-03
DNA metabolism	BP	14	10.87	ns	39	20.91	3.35E-02
Other RNA-binding protein	MF	11	5.8	ns	25	11.15	3.66E-02
DNA repair	BP	8	5.1	ns	23	9.82	4.28E-02
KRAB box transcription factor	MF	37	17.7	6.40E-03	53	34.03	ns

ns, not significant; BP, biological process; MF, molecular function; PA, pathway; PBL, peripheral blood lymphocyte; LCL, lymphoblastoid cell line; MRs, methylated regions.

LCLs are generated by transforming peripheral B lymphocytes with EB viral infection. This could affect the DNA methylation patterns. If these changes in the DNA methylation pattern in LCLs occur in a small proportion or at specific regions, LCLs could be used for DNA methylation analysis with cautious interpretation of the results. In this study, we performed a comprehensive DNA methylation analysis using PBL and LCL sets from the same individuals. A comparison of the global methylation level by LUMA revealed that the direction of the changes was not consistent across samples. These results suggest that LCLs are not a suitable alternative for PBLs for measuring global DNA methylation levels.

The global DNA methylation level of PBLs is also altered in both directions with aging.[18,19] Thus, global methylation levels in the peripheral tissues are likely to be unstable upon changes in the internal or external environment.

In the comparison of genome-wide methylation patterns using the Affymetrix Human promoter array, the correlation coefficients among LCLs were significantly lower than those among PBLs. This result was consistent with the results of a previous study in reference 7, and indicated that the DNA methylation

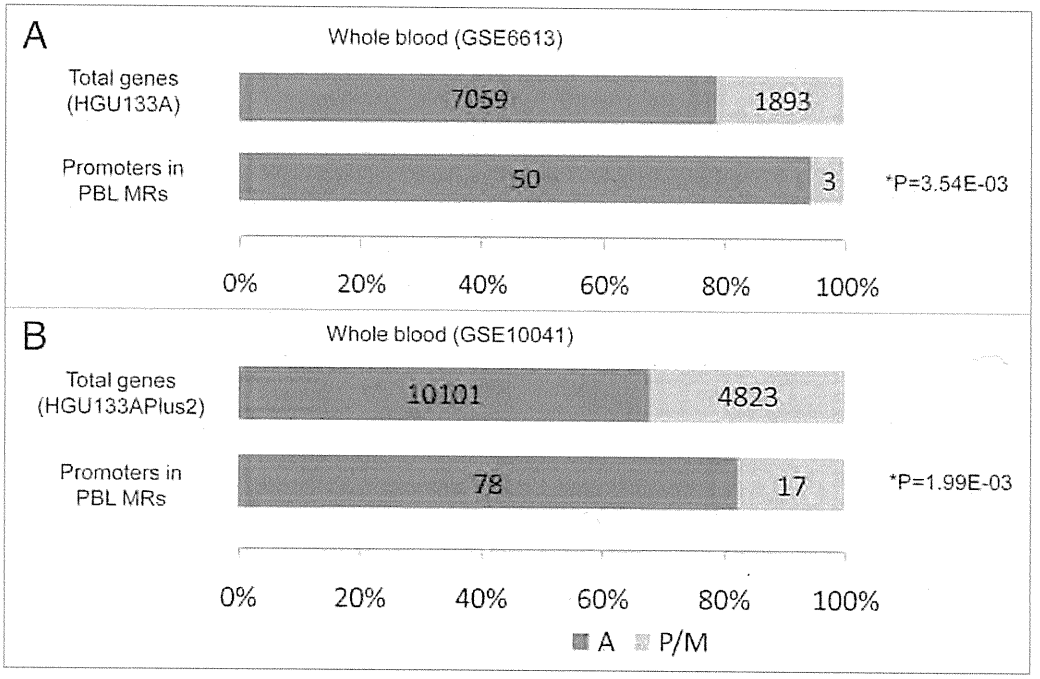

Figure 3. Effect of methylation in promoter regions overlapping with CpG islands on gene expression in PBLs. The numbers of genes containing at least one probe with present or marginal flags, as well as that of genes whose all probes were called as absent, are indicated. If all samples across the chosen study showed absent flags with respect to a certain probe set, we considered this "absent," and "present" probes were determined similarly. If one gene had both probe sets of present/marginal and absent, the gene was classified as an expressed gene. (A) HGU133A platform (GSE6613 (the number of control samples N = 22)[14]), (B) HGU133plus2.0 platform (GSE10041 (N = 23)[15]). Fisher's exact test p values are given. A: genes with absent probes, P/M: genes with present or marginal probes, N = number of control samples.

profile was not completely conserved in LCLs. This study showed that methylation status in LCLs was correlated with that in PBLs from the same individuals. Although this finding should be confirmed in a larger sample set, DNA methylation profiles could be at least partly maintained after EB virus transformation. In addition, among the 1,510 methylated regions in PBLs, 1,379 regions were also detected as methylated regions in LCLs. Thus, most of the promoter methylation regions in PBLs were maintained in LCLs.

We expectedly found an association between DNA methylation in promoter regions overlapping with CpG islands and gene silencing in both PBLs and LCLs. Grafodatskaya et al. hypothesized that random methylation occurs in LCLs preferentially in genes that are not important for cell survival. However, the present results of gene ontology analysis in LCL-specific MRs showed that methylation in LCLs occurs in similar genes to those methylated in PBLs.

Although the direction of promoter methylation changes in individual LCL samples was not consistent, hypermethylation was overall more predominant than hypomethylation in LCLs. In any case, it should be cautioned that methylation patterns in LCLs do not always reflect that in PBLs in the study of human diseases.

Limitation

Although we used PBLs and LCLs to identify changes in the methylation patterns in LCLs, B lymphocytes are more suitable than PBLs because their use avoids the effect of cellular heterogeneity within PBLs. In addition, LCLs constitute a subset of B lymphocytes selected by the EB virus as a host, and methylation patterns might depend on the B lymphocyte subset. Further studies are required to exclude these confounding factors. Because we used only low-passage LCLs without freezing, the effects of passage number and freezing cycles on changes in the methylation pattern in LCLs were not evaluated. We could perform LUMA assay only in three of four sets of PBL because of the limited amount of DNA left. Analysis of larger number of DNA samples would be helpful to elucidate global methylation change in LCLs in the future. In addition, larger number of samples is needed to test the validity of a LCL as a representative of PBL in an individual.

Materials and Methods

Samples. For the LUMA, we used three sets of PBLs and LCLs obtained from the same unrelated healthy Japanese individuals, 29-(C1) and 52-(C4) year old males and a 25 year-old female (C3). The LCL DNA derived from a healthy 27 year-old Japanese male was used to prepare standard DNA samples as described below. For methylation analysis using promoter tiling arrays, we used one additional set of PBLs and LCL from a 25 year-old healthy Japanese female (C2). We used another one set of PBLs and LCLs from a 45-year-old healthy Japanese male for bisulfite sequencing. This study was approved by the Research Ethics